

Effect of rainfall and fire frequency on tree–grass dynamics: Capturing the forest–savanna distributions along biogeographic gradients

A. Tchuinté Tamen^{1*}, P. Couteron^{2,4}, Y. Dumont^{3,4,5}

¹*Faculty of Science, University of Yaoundé I, Cameroon*

²*IRD, UMR AMAP, Montpellier, France*

³*CIRAD, UMR AMAP, Pretoria, South Africa*

⁴*AMAP, University of Montpellier, CIRAD, CNRS, INRA, IRD, Montpellier, France*

⁵*Department of Mathematics and Applied Mathematics, University of Pretoria, South Africa*

February 19, 2018

Abstract

In this work, we improve a previous minimalistic tree–grass savanna model by taking into account water availability, in addition to fire, since both factors are known to be important for shaping savanna physiognomies along a climatic gradient. As in our previous models, we consider two nonlinear functions of grass and tree biomasses to respectively take into account grass–fire feedbacks, and the response of trees to fire of a given intensity. The novelty is that rainfall is taken into account in the tree and grass growth functions and in the biomass carrying capacities. Then, we derive a qualitative analysis of the ODE model, showing existence of equilibria, and studying their stability conditions. We also construct a two dimension bifurcation diagram based on rainfall and fire frequency. This led to summarize different scenarios for the model including multi–stabilities that are proven possible. Next, to bring more realism in the model, pulsed fire events are modelled as part of an IDE (Impulsive differential Equations) system analogous to the ODE system. Numerical simulations are provided and we discuss some important ecological outcomes that our ODE and IDE models are able to predict. Notably, the expansion of forest into tree–poor physiognomies (grassland and savanna) is systematically predicted when fire return period increases, especially in mesic and humid climatic areas.

Keywords: Tree–grass interactions; Rainfall; Fires; Ordinary differential equations; Impulsive differential equations; Multi–stability; Periodic solutions; Bifurcation diagram.

1 Introduction

Savannas, as broadly defined as systems where tree and grass coexist (Scholes and Archer, 1997), occupy about 20% of the Earth land surface and are observed in a large range of Mean Annual Precipitation (MAP). In Africa, they particularly occur between 100 mm and 1500 mm (and sometimes

*Corresponding author: alexis.tchuinte@yahoo.fr

more) of total mean annual precipitation (Lehmann et al., 2011; Baudena and Rietkerk, 2013), that is along a precipitation gradient leading from dense tropical forest to desert. There is widespread evidence that fire and water availability are variables which can exert determinant roles in mixed tree-grass systems (Scholes and Archer, 1997; Van Langevelde et al., 2003; Sankaran et al., 2005; Staver and Levin, 2012; Baudena et al., 2014). Fires kill aerial parts of seedlings and shrubs while tree parts above the 'flame zone' are little affected (Scholes, 2003). On the other hand, water availability is considered to be the primary determinant of biomass production and indirectly of vegetation dynamics and structure in savannas (Frost et al., 1986; Sankaran et al., 2005; Abbadie et al., 2006; Bond, 2008). Moreover, empirical studies showed that vegetation properties such as biomass, leaf area, net primary production, maximal tree height and annual maximum standing crop of grasses vary along gradients of precipitation (Penning de Vries and Djitéye, 1982; Abbadie et al., 2006). It is widely accepted that water availability directly limits woody vegetation in the driest part of the rainfall gradient (Frost et al., 1986; Sankaran et al., 2005; Bond, 2008). Along the rest of this gradient, rainfall is known to influence indirectly the fire regime through what can be referred to as the grass-fire feedback (Higgins et al., 2010; Staver et al., 2011b; Baudena et al., 2014): grass biomass that grows during rainfall periods is fuel for fires occurring in the dry months. Sufficiently frequent and intense fires are known to prevent or at least delay the development of woody vegetation (Van Wilgen et al., 2004; Bond et al., 2005; Govender et al., 2006), thereby preventing trees and shrubs to depress grass production through shading. The grass-fire feedback is widely acknowledged in literature as a force able to counteract the asymmetric competition of trees onto grasses, at least for climatic conditions within the savanna biome that enables sufficient grass production during wet months.

Dynamical processes underlying savanna vegetation have been the subject of many models. Some of them explicitly considered the influence of soil water resource on the respective productions of grass and woody vegetation components (Walker et al., 1981; Walker and Noy-Meir, 1982; Rietkerk et al., 1997; Rietkerk et al., 2002; Van De Koppel and Rietkerk, 2000; Van Langevelde et al., 2003; D'Odorico et al., 2006; De Michele et al., 2008; Accatino et al., 2010; De Michele et al., 2011; Yu and D'Odorico, 2014). Most of these models also incorporated the grass-fire positive feedback, several of them distinguishing fire-sensitive small trees and shrubs from non-sensitive large trees (Higgins et al., 2000; Beckage et al., 2009; Baudena et al., 2010; Staver et al., 2011b; Yatat et al., 2014), while the rest stuck to the simplest formalism featuring just grass and tree state variables (Van Langevelde et al., 2003; D'Odorico et al., 2006; Higgins et al., 2010; Accatino et al., 2010; Beckage et al., 2011; Yu and D'Odorico, 2014; Tchuinté Tamen et al., 2014). Models featuring the grass-fire feedbacks have shown that physiognomies displaying tree-grass coexistence (i.e. savannas) may be stable (Van Langevelde et al., 2003; D'Odorico et al., 2006; Baudena et al., 2010; Accatino et al., 2010; Yatat et al., 2014; Tchuinté Tamen et al., 2014) as well as more 'trivial' equilibria such as desert, dense forest or open grassland. Some models also predict alternative stable physiognomies under similar rainfall conditions (Accatino et al., 2010; Staver et al., 2011b; Yatat et al., 2014; Tchuinté Tamen et al., 2014), a feature that is suggested as plausible by remote-sensing studies (Favier et al., 2012; Hirota et al., 2011; Cuni-Sanchez et al., 2016) as well as field observations of contrasted mosaics (see Fig. 1). However, just a subset of the published models addressed the entire rainfall gradient of the savanna biome (Accatino et al., 2010; Higgins et al., 2010; Baudena et al., 2010; De Michele et al., 2011; Beckage et al., 2011; Yu and D'Odorico, 2014). The ability to predict all the physiognomies that are suggested by observations as possible stable or multi-stable outcomes was not established but for Accatino et al., 2010.



(a)



(b)

Figure 1: (a) Photo of forest–grassland boundary in Mpem & Djim National Park, Central Cameroon. (b) An abrupt Forest–savanna (grassland) mosaics in Ayos, Cameroon.

The need to understand vegetation dynamics over very large territories for which information to calibrate models is scarce makes however desirable simple and robust models. The Accatino et al., 2010 model which built on De Michele et al., 2008 was pioneering in the sense that it allowed these authors to provide a "broad picture", by delimitating stability domains for a variety of possible vegetation equilibria as functions of gradients in rainfall and fire intensity. This result was especially interesting that the considered model was sufficiently simple (two vegetation variables, i.e. grass and tree covers) to provide analytical forecasts. However, results from Accatino et al., 2010 were questionable regarding the role of fire return time. In fact, all over the rainfall gradient their model predicted that decreasing fire frequency would lead to increase in woody cover which contradicts most of empirical knowledge on the subject. The features of the model that led to this problem were barely debated in the ensuing publications. And more recent papers instead either devised more complex models or shift to stochastic modelling (D’Odorico et al., 2006; Beckage et al., 2011). Such models did not allow much analytical exploration of their fundamental properties.

On the other hand, criticism against the ODE modelling (Accatino and De Michele, 2016; Accatino et al., 2016) pertinently argued that fires do not exert a continuous forcing on vegetation through time but rather destroy large shares of biomass through punctual events. Tchuinté Tamen et al., 2017 showed that the impulsive differential (IDE) framework can provide an interesting trade-off by modelling fires as punctual events albeit preserving the tractability of ODE equations that governs vegetation growth in inter-fire periods. They devised an IDE model that not only acknowledged punctual fires, but also reworked the way in which grass-fire feedback and fire im-

impact on trees were modelled. Notably, fire intensity became a sigmoidal function of grass biomass (Tchuinté Tamen et al., 2016; Yatat et al., 2016), while a decreasing non-linear function of woody biomass was introduced to express fire impact on woody plants. The behavior of this IDE model proved immune to the increasing relationship between fire frequency and woody biomass that crippled earlier modelling efforts (Tchuinté Tamen et al., 2017). But the relationship between modelling results and rainfall remained indirect through model parameters that changed according to three main climatic zones (arid, mesic, humid) in the savanna biome.

In the present paper, we will explicitly express the growth of both woody and herbaceous vegetation as functions of the mean annual rainfall, with the aim to study model predictions in direct relation to rainfall and fire frequency gradients. We will show that the two-variable ODE framework is not irrelevant per se and that an appropriate formulation of the grass-fire-tree retroaction loop makes it able to provide meaningful predictions while remaining fully analytically tractable. Through simulations, we will also show that the analogous ODE and IDE versions of our model qualitatively agree regarding stability domains, though diverging in several particular aspects. Through the present contribution we aim at proposing a framework for modelling vegetation in the savanna biome, that is both minimal (in terms of state variables and parameters) and generic in the sense that it does not pertain to particular locations (Accatino and De Michele, 2016). In so doing, we aim to show that our minimalistic tree-grass dynamical model is able to provide at broad scales, a more consistent array of sensible predictions of possible vegetation physiognomies than previous ODE tree-grass frameworks. For instance, to our knowledge, existing models with only two vegetation state variables do not allow to capture the well-known fact that decreasing fire return period never leads to an increase of woody biomass whatever the place along a climatic gradient and especially in mesic and humid climatic conditions.

We aim to account for a wide range of physiognomies and dynamical outcomes of the system at both regional and continental scales by relying on a simple model that explicitly address some essential processes that are: (i) limits put by rainfall on vegetation biomass and growth (ii) asymmetric interactions between woody and herbaceous plant life forms, (iii) positive feedback between grass biomass and fire intensity and decreased fire impact with tree height.

Through integration of rainfall in plant growth and carrying capacity, the new IDE model introduced here is an extension of our previous impulsive model (Tchuinté Tamen et al., 2017). An idiosyncrasy of our minimalistic tree-grass model is that we considered the fire induced mortality on woody biomass by mean of two independent non-linear functions, namely ω (see (1)) and ϑ (see (2)). Considering these two functions (Tchuinté Tamen et al., 2017; Tchuinté Tamen, 2017), we showed that the previous model substantially improve previously published results on tree-grass dynamical systems. For example we showed that increasing fire return period systematically leads the system to switches from grassland or savanna to forest (forest encroachment). This result is entirely consistent with field observations (Bond et al., 2005; Bond and Parr, 2010; Favier et al., 2012; Jeffery et al., 2014). The novelty in the present IDE model is that we combine pulsed fire and rainfall in order to study how the frequency of pulsed fires change the vegetation along a rainfall gradient. Assuming that fires are periodic in time and that growths and carrying capacities of grass and tree vary as nonlinear functions of rainfall, we aim to reproduce the whole set of physiognomies observable along the rainfall gradients leading in Africa from forests to deserts.

This paper is organized as follows. Section 2 presents modelling framework of the ODE and IDE models. Section 3 gives the main theoretical results of the ODE and IDE models. In section 4 a 2D-bifurcation diagram in the rainfall-fire frequency space is given and numerical simulations

are also provided to discuss some important ecological scenarios. Finally, the paper ends with a conclusion and acknowledgements.

2 Modelling frameworks: ODE and IDE

The model considers the following assumptions.

- (A1) Within the framework of tree-grass interactions, most models used vegetation state variables that corresponded to cover fractions that sum to one or less (De Michele et al., 2008; Baudena et al., 2010; Accatino et al., 2010; Staver et al., 2011b; De Michele et al., 2011; Yu and D’Odorico, 2014). It implicitly means assuming that vegetation components are mutually exclusive. Many field studies in fact showed that shrub and grass biomasses often exist under a tree crown (e.g., Scholes and Archer, 1997; Abbadie et al., 2006; Moustakas et al., 2013).

In this work as well as in our previous studies (Tchuinté Tamen et al., 2014; Tchuinté Tamen et al., 2016; Tchuinté Tamen et al., 2017) we use biomasses as state variables since it allows a more straightforward link with field measurements (especially for grasses) and with emerging sources of remotely-sensed data as woody biomass estimates from radar backscattering (Mermoz et al., 2015).

- (A2) The annual productions of grass and trees are assumed to be non-linear and saturating functions of the mean annual precipitation (MAP), here noted \mathbf{W} (in millimeter per year, mm.yr^{-1}). Following van de Koppel et al., 1997, Higgins et al., 2010 and Van Nes et al., 2014 a Monod equation is judged an adequate form to describe relationships between growth and rainfall since it is consistent with empirical data (e.g., Whittaker, 1975, see also fig. 4.6.3, p 191 in Penning de Vries and Djitéye, 1982). We assume that $\frac{\gamma_G \mathbf{W}}{b_G + \mathbf{W}}$ and $\frac{\gamma_T \mathbf{W}}{b_T + \mathbf{W}}$ are annual productions of grass and tree biomasses respectively, where γ_G and γ_T (in yr^{-1}) express maximal growths of grass and tree biomasses respectively, half saturations b_G and b_T (in mm.yr^{-1}) determine how quickly growth increase with water availability.

The estimate value $\gamma_G = 2$ is obtained using data from Penning de Vries and Djitéye, 1982 (see figure 4.6.3 (a), p 191). The value $b_G = 501 \text{ mm.yr}^{-1}$ is deduced using data from UNESCO, 1981 (see fig 7, p 599). $\gamma_T = 0.15$ and 0.533 are estimated using data from Chidumayo, 1990 and Menaut and Cesar, 1979 respectively. The value $b_T = 1192 \text{ mm.yr}^{-1}$ is deduced from Abbadie et al., 2006. Finding $b_G < b_T$ is not unrealistic but has been barely mentioned and discussed in literature. Though Scholes and Walker, 1993 (see fig 1.1, page 3) suggested that grass and tree production may diverge along moisture gradients. Accatino et al., 2010 considered that vegetation growths are linear functions of soil moisture, however, the non-linear relationship between soil-water and biomass production is widely observed in the field (Mordelet, 1993; Le Roux and Bariac, 1998; Simioni et al., 2003; House et al., 2003).

- (A3) We assume that carrying capacities of grass $K_G(\mathbf{W})$ and tree $K_T(\mathbf{W})$ are increasing and bounded functions of water availability \mathbf{W} . There are empirical data sets (e.g. UNESCO, 1981; Sankaran et al., 2005; Bucini and Hanan, 2007; Staver et al., 2011b; Staver et al., 2011a; Favier et al., 2012; Lewis et al., 2013) which showed that maximum potential tree biomass increases with rainfall. For example, Sankaran et al., 2005 analysed tree cover for 850 field

locations in African savannas along a range of increasing rainfall. They found that maximum tree cover increases from 0 to 80% as mean annual precipitation (MAP) increases from ~ 100 mm to ~ 650 mm, value above which closed canopy (80% cover) can be observed in the absence of disturbance. Other studies have been done to explain the changes of tree cover against MAP at a continental scale (see Bucini and Hanan, 2007 and Favier et al., 2012). Bucini and Hanan, 2007 used MODIS (Moderate Resolution Imaging Spectroradiometer) data and they showed that average tree cover increases asymptotically with rainfall.

From those previous studies, relationship between maximum tree biomass vs. rainfall can be expressed as increasing and saturating functions (see fig 2 (a) in Favier et al., 2012). To determine the form of K_T , we use field plot data from Higgins et al., 2010 and Lewis et al., 2013 (see also Fig. 2) and consider that K_T might follow a sigmoid function. To fit the data we use the following function $K_T(\mathbf{W}) = \frac{c_T}{1 + d_T e^{-a_T \mathbf{W}}}$, where c_T (in $\text{t}\cdot\text{ha}^{-1}$) stands for maximum value of the tree biomass carrying capacity, a_T (mm^{-1}yr) controls the steepness of the curve, and d_T controls the location where is the inflection point. Note that the function K_T is rationally analogue to the Holling type III functional response. We used the nonlinear quantile regression (Koenker and Park, 1996), as implemented in the "quantreg" library of the R program and we have $c_T = 498.6 \text{ t}\cdot\text{ha}^{-1}$, $d_T = 106.7$, and $a_T = 0.0045 \text{ mm}^{-1}\text{yr}$. Concerning the grass biomass standing crop, K_G , we used empirical field data from Braun, 1972a and Braun, 1972b (see Fig. 2 and see also UNESCO, 1981 page 599), Menaut and Cesar, 1979, and Abbadie et al., 2006, and we consider the following function: $K_G(\mathbf{W}) = \frac{c_G}{1 + d_G e^{-a_G \mathbf{W}}}$, where c_G (in $\text{t}\cdot\text{ha}^{-1}$) denotes the maximum value of the grass biomass carrying capacity, a_G (mm^{-1}yr) controls the steepness of the curve, and d_G controls the location where is the inflection point. We have the following values: $c_G = 17.06 \text{ t}\cdot\text{ha}^{-1}$, $d_G = 14.73$, and $a_G = 0.0029 \text{ mm}^{-1}\text{yr}$. For the first time to our knowledge we aimed at characterizing the maximal possible woody biomass for both savanna and forest contexts.

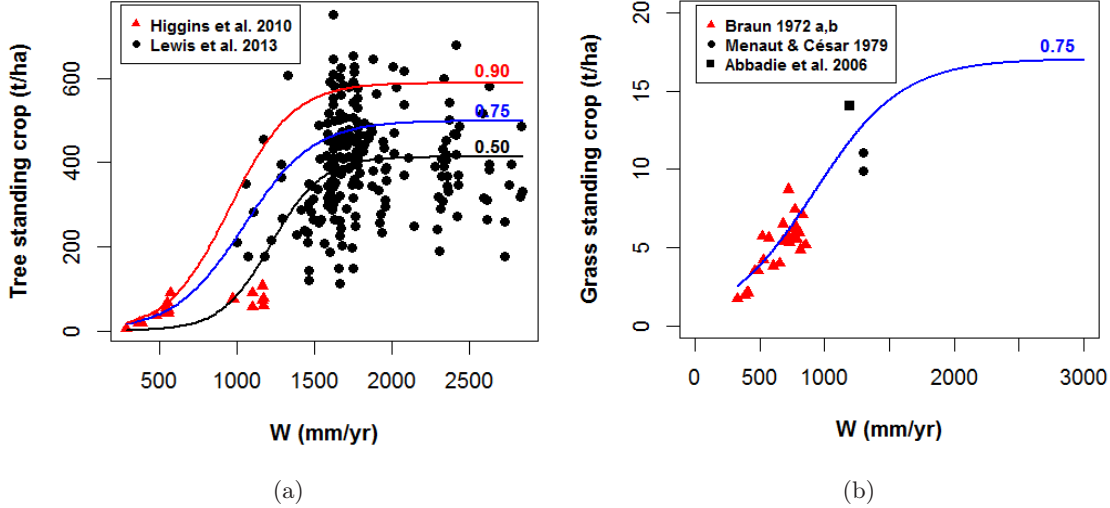


Figure 2: (a) Maximum tree biomass production K_T versus rainfall. Data are from Higgins et al., 2010 and Lewis et al., 2013. (b) Maximum grass biomass production K_G versus rainfall. Data are from Menaut and Cesar, 1979; Braun, 1972a; Braun, 1972b (see also UNESCO, 1981 page 599) and Abbadie et al., 2006.

(A4) Like in our previous works (Tchuinté Tamen et al., 2014; Tchuinté Tamen et al., 2016; Tchuinté Tamen et al., 2017), we assume that the fire intensity noted ω is an increasing and bounded function of the grass biomass given as follows:

$$\omega(G) = \frac{G^\theta}{G^\theta + \alpha^\theta}, \quad (1)$$

where, G in tons per hectare ($\text{t}\cdot\text{ha}^{-1}$) is grass biomass, α is the value takes by G when fire intensity is half its maximum, and the integer θ determines the steepness of the sigmoid. The nonlinear form of ω is in agreement with recent models of savanna systems such as Staver et al., 2011b (for a Holling type III form) and the works of Tchuinté Tamen et al., 2014; Yatat et al., 2014; Tchuinté Tamen et al., 2016; Yatat et al., 2016; Tchuinté Tamen et al., 2017 (for generic sigmoidal forms). The parameter α is estimated as $\alpha = 1.5 \text{ t}\cdot\text{ha}^{-1}$ (see fig 3 in Govender et al., 2006). In the rest of this article, we set $\theta = 2$.

Accatino et al., 2010 along with other authors assumed that fire intensity increases linearly with fuel load (i.e., grass biomass). But, nonlinear forms (e.g., sigmoidal shape) of fire intensity functions agree with real ecological situations. Although Staver et al., 2011b suggested that the nonlinear response function is a sufficient mechanism to let forest and savanna be alternative stable states, they made some peculiar assumptions (e.g. both saplings and trees die and revert to grass in proportion to their cover). And their model is not able to predict as equilibria the full set of vegetation physiognomies that are observed along the whole climatic gradient, that features desert and wet tropical forest in addition to grassland and savanna. The central issue is that most savanna models (including ecohydrologic ones) are specific to

certain climate zones. As a consequence they can account neither for all the physiognomies which are observed nor for all the multiple stable states which can be hypothesized considering the contrasted physiognomies observed under similar climatic conditions.

- (A5) Fire-induced tree/shrub mortality, noted ϑ is assumed to be a decreasing, non-linear function of tree biomass. In this paper as in Tchuinté Tamen et al., 2017, we assume that fires affect differently large and small trees since fires with high intensity (flame length $> 2\text{m}$) cause greater mortality of shrubs and topkill of trees while fires of lower intensity (flame length $< 2\text{m}$) kill only shrubs and subshrubs (Trollope et al., 2002; Hoffmann and Solbrig, 2003; Higgins et al., 2007). It is evident that tree biomass and height are linked by increasing relationships. Therefore, as in Tchuinté Tamen et al., 2017, ϑ is expressed as follows:

$$\vartheta(T) = \lambda_{fT}^{min} + (\lambda_{fT}^{max} - \lambda_{fT}^{min})e^{-pT}, \quad (2)$$

where, T in tons per hectare ($\text{t}\cdot\text{ha}^{-1}$) stands for tree biomass, λ_{fT}^{min} (in yr^{-1}) is minimal loss of tree biomass due to fire in systems with a very large tree biomass, λ_{fT}^{max} (in yr^{-1}) is maximal loss of tree/shrub biomass due to fire in open vegetation (e.g. for an isolated woody individual having its crown within the flame zone), p (in $\text{t}^{-1}\cdot\text{ha}$) is proportional to the inverse of biomass suffering an intermediate level of mortality. To parametrize ϑ , we used experimental data from Trollope et al., 2002 on the effects of height on the topkill rate of individual trees and shrubs in the Kruger National Park in South Africa, and in the central highlands of Kenya. We estimated biomass from height using an allometric equation provided by West et al., 2009 stating that at individual tree level, the total above-ground biomass (t/ha) is a power function of height (m) with an exponent of 4. The estimated parameters of ϑ are: $\lambda_{fT}^{min} = 0.05 \text{ yr}^{-1}$, $\lambda_{fT}^{max} = 0.9 \text{ yr}^{-1}$ and $p = 0.03 \text{ t}^{-1}\cdot\text{ha}$. Notice that Higgins et al., 2007 considered that $\lambda_{fT}^{min} < 0.05$ and $\lambda_{fT}^{max} > 0.9$.

The above considerations motivate us to introduce a minimalistic eco-hydrological model under the framework of the following set of nonlinear ordinary differential equations :

$$\begin{cases} \frac{dG}{dt} = \frac{\gamma_G \mathbf{W}}{b_G + \mathbf{W}} G \left(1 - \frac{G}{K_G(\mathbf{W})} \right) - \delta_G G - \eta_{TG} T G - \lambda_{fG} f G, \\ \frac{dT}{dt} = \frac{\gamma_T \mathbf{W}}{b_T + \mathbf{W}} T \left(1 - \frac{T}{K_T(\mathbf{W})} \right) - \delta_T T - f \vartheta(T) \omega(G) T, \\ G(0) = G_0, T(0) = T_0, \end{cases} \quad (3)$$

where,

- G and T (in $\text{t}\cdot\text{ha}^{-1}$) stand for grass and tree biomasses respectively;
- \mathbf{W} (in $\text{mm}\cdot\text{yr}^{-1}$) is the mean annual precipitation MAP parameter.
- G_0 and T_0 (in $\text{t}\cdot\text{ha}^{-1}$) are initial conditions of grass and tree biomasses respectively;
- δ_G and δ_T express respectively the rates of grass and tree biomasses loss by herbivores (grazing and/or browsing) or by human action;

- η_{TG} denotes the asymmetric influence of trees on grass for light (shading) and resources (water, nutrients) which result in competitive or facilitative influences;
- $f = \frac{1}{\tau}$ is the fire frequency, where τ is the fire return period;
- λ_{fG} is the specific loss of grass biomass due to fire.

In savanna ecosystems, it is widely observed that disturbances such as fires act in punctual way such that they consume tree/shrub and grass biomasses over a short lapse of time (House et al., 2003; Scheiter, 2009). In our previous works (Tchuinté Tamen et al., 2016; Tchuinté Tamen et al., 2017), we proposed a tree–grass savanna model that considers fire occurrence and impact as pulse periodic events through impulsive differential equations (IDE). The IDE framework (Lakshmikantham et al., 1989; Bainov and Simeonov, 1993) is more realistic though keeping amenable to in-deep analytical investigations of the models (Tchuinté Tamen et al., 2016; Yatat et al., 2016; Tchuinté Tamen et al., 2017). Moreover, we showed that modelling fire as pulse events allow more diverse and interesting outcomes than modelling fire as a time-continuous external forcing. For instance, we showed that approximating fire regime as periodic let analytically investigating the possibility of periodic solutions and various bistabilities. Assuming periodic pulsed fires in system (3), we obtain the following impulsive differential equation:

$$\left\{ \begin{array}{l} \frac{dG}{dt} = \frac{\gamma_G \mathbf{W}}{b_G + \mathbf{W}} G \left(1 - \frac{G}{K_G(\mathbf{W})} \right) - \delta_G G - \eta_{TG} T G, \\ \frac{dT}{dt} = \frac{\gamma_T \mathbf{W}}{b_T + \mathbf{W}} T \left(1 - \frac{T}{K_T(\mathbf{W})} \right) - \delta_T T, \end{array} \right\}, t \neq t_n, \quad (4)$$

$$\left\{ \begin{array}{l} G(t_n^+) - G(t_n) = -\lambda_{fG} G(t_n), \\ T(t_n^+) - T(t_n) = -\vartheta(T(t_n))\omega(G(t_n))T(t_n), \end{array} \right\}, t = t_n, n = 1, 2, \dots, N_\tau,$$

with the initial conditions

$$G(t_0) = G_0, T(t_0) = T_0, \quad (5)$$

where, $\tau = \frac{1}{f}$ is the period between two consecutive fires and f is the frequency of fire, N_τ is a countable number of fire occurrences, $t_n = n\tau$, $n = 1, 2, \dots, N_\tau$, are called moments of impulsive effects of fire, and satisfy $0 \leq t_1 < t_2 < \dots < t_{N_\tau}$, $G(t_n^+)$ and $T(t_n^+)$ are grass and tree biomasses instantly after an impulsive fire.

Remark 2.1 (i) *It is important to note that the impulsive differential system (4) completes our previous IDE model developed and studied in Tchuinté Tamen et al., 2017. The novelty is that, here we consider that annual productions and carrying capacities of grass and tree biomasses vary according to the mean annual precipitation \mathbf{W} while in Tchuinté Tamen et al., 2017, they were assumed to be constant. Indeed, as mentioned in assumptions (A2) and (A3), there are empirical data sets which support the evidence of relationships between rainfall and annual productions and carrying capacities of grass and tree biomasses respectively (e.g., for biomass productions see Whittaker, 1975, see fig 7 of page 599 in UNESCO, 1981, see also fig. 4.6.3*

of page 191 in Penning de Vries and Djitéye, 1982 and for maximum potential biomasses see UNESCO, 1981 page 599; Abbadie et al., 2006; Higgins et al., 2010; Lewis et al., 2013).

(ii) Since system (4) and the model developed and studied in Tchuinté Tamen et al., 2017 are almost similar, the readers are referred to appendices in Tchuinté Tamen et al., 2017 for the proofs of theoretical results. Accordingly, the demonstrations are deduced by replacing the constant parameters of productions (γ_G and γ_T) and carrying capacities (K_G and K_T) by non-linear, increasing and bounded functions of MAP (\mathbf{W}) as given above in (A2) and (A3) respectively. However, the ODE model (3) is proposed and studied here for the first time.

3 Analytical results

3.1 The ODE model

The right-hand side of system (3) is \mathcal{C}^1 i.e., continuously differentiable. Then, from the Cauchy-Lipschitz theorem, system (3) has a unique maximal solution. In the ecological point of view, since the variables of system (3) represent the biomasses, each variable must stay positive and must be bounded during the time evolution (i.e., the system is said to be biologically well-behaved). Note that a solution with initial conditions in \mathbf{R}_+^2 stays in \mathbf{R}_+^2 since it can not cut the y-axis (vertical null line) and the x-axis (horizontal null line). Set

$$\Gamma = \{(G, T) \in \mathbf{R}_+^2 : G \leq K_G(\mathbf{W}), T \leq K_T(\mathbf{W})\},$$

It is easy to verify that the sub-set Γ is positively invariant and attracting with respect to system (3). It means that all trajectories of system (3) that start in Γ remain positive and they do not tend to infinity with increasing time.

Set

$$\begin{cases} g_G(\mathbf{W}) = \frac{\gamma_G \mathbf{W}}{b_G + \mathbf{W}}, \\ g_T(\mathbf{W}) = \frac{\gamma_T \mathbf{W}}{b_T + \mathbf{W}}, \end{cases} \quad (6)$$

$$\begin{cases} \mathcal{R}_{\mathbf{W}}^1 = \frac{g_T(\mathbf{W})}{\delta_T}, \\ \mathcal{R}_{\mathbf{W}}^2 = \frac{g_G(\mathbf{W})}{\delta_G + \lambda_{fG} f}, \end{cases} \quad (7)$$

and

$$\begin{cases} T^* = K_T(\mathbf{W}) \left(1 - \frac{1}{\mathcal{R}_{\mathbf{W}}^1}\right), \\ G^* = K_G(\mathbf{W}) \left(1 - \frac{1}{\mathcal{R}_{\mathbf{W}}^2}\right). \end{cases} \quad (8)$$

System (3) has the following trivial equilibria:

- a bare soil equilibrium $\mathbf{E}_0 = (0, 0)$.
- a forest equilibrium $\mathbf{E}_F = (0, T^*)$ which exists when $\mathcal{R}_{\mathbf{W}}^1 > 1$.

- a grassland equilibrium $\mathbf{E}_G = (G^*, 0)$ which exists when $\mathcal{R}_{\mathbf{W}}^2 > 1$.

Let us set:

$$a = \frac{g_T(\mathbf{W})}{K_T(\mathbf{W})}T^*, \quad b = \frac{g_G(\mathbf{W})g_T(\mathbf{W})}{\eta_{TG}K_G(\mathbf{W})K_T(\mathbf{W})}G^*, \quad c = \frac{b}{G^*}, \quad d = f\lambda_{fT}^{\min}, \quad \lambda = f(\lambda_{fT}^{\max} - \lambda_{fT}^{\min}) \times e^{-p \frac{g_G(\mathbf{W})G^*}{\eta_{TG}K_G(\mathbf{W})}}$$

and $\alpha = p \frac{g_G(\mathbf{W})}{\eta_{TG}K_G(\mathbf{W})}$, where G^* is given by (8).

The existence of the positive savanna equilibrium is given in theorem 3.1.

Theorem 3.1 (*Existence of the savanna equilibrium*)

Table 1 summarizes the conditions of existence the savanna equilibrium.

Table 1: Existence of the savanna equilibrium

$c - \lambda\alpha$	$a - b - d - \lambda$	$a - b$	Number of savanna equilibria
< 0	> 0	> 0	0 or 1
	or	< 0	0 or 2
< 0	$\begin{cases} \leq 0 \\ \geq 0 \end{cases}$	> 0	0 or 1
		< 0	0 or 2
	< 0	> 0	0, 1 or 3
		< 0	0 or 2

Proof: See appendix A, page 27.

We now study the stability of the previous equilibria. Concerning the stability of the trivial equilibria \mathbf{E}_0 , \mathbf{E}_G , and \mathbf{E}_F , theorem 3.2 holds. Set

$$\mathcal{R}_F = \frac{g_G(\mathbf{W})}{\eta_{TG}T^* + \delta_G + \lambda_{fG}f}, \quad \text{and} \quad \mathcal{R}_G = \frac{g_T(\mathbf{W})}{\delta_T + \lambda_{fT}^{\max}f\omega(G^*)}. \quad (9)$$

Straightforward computations lead to the following theorem:

Theorem 3.2 (*Stability of trivial equilibria*)

- (1) The desert equilibrium $\mathbf{E}_0 = (0, 0)$ is locally asymptotically stable (LAS) when $\mathcal{R}_{\mathbf{W}}^1 < 1$ and $\mathcal{R}_{\mathbf{W}}^2 < 1$.
- (2) The grassland equilibrium $\mathbf{E}_G = (G^*, 0)$ is LAS when $\mathcal{R}_G < 1$.
- (3) The forest equilibrium $\mathbf{E}_F = (0, T^*)$ is LAS when $\mathcal{R}_F < 1$.

Remark 3.1 *It is to be noted that the existence of \mathbf{E}_F or \mathbf{E}_G destabilizes the desert equilibrium \mathbf{E}_0 .*

Let $\mathbf{E}_S = (G_*, T_*)$ a savanna equilibrium. Define

$$\left\{ \begin{array}{l} \mathcal{R}_*^1 = \frac{\frac{g_G(\mathbf{W})}{K_G(\mathbf{W})}G^* + \frac{g_T(\mathbf{W})}{K_T(\mathbf{W})}T^* - \vartheta'(T_*)f\omega(G_*)T_*}{2\left(\frac{g_G(\mathbf{W})}{K_G(\mathbf{W})}G^* + \frac{g_T(\mathbf{W})}{K_T(\mathbf{W})}T^*\right) + \eta_{TG}T_* + f\omega(G_*)\vartheta(T_*)}, \\ \mathcal{R}_*^2 = \frac{\frac{g_G(\mathbf{W})g_T(\mathbf{W})}{K_G(\mathbf{W})K_T(\mathbf{W})}G^*T^* + A_*B_* - \vartheta'(T_*)\frac{g_G(\mathbf{W})}{K_G(\mathbf{W})}G^*f\omega(G_*)T_*}{\frac{g_G(\mathbf{W})}{K_G(\mathbf{W})}G^*B_* + \frac{g_T(\mathbf{W})}{K_T(\mathbf{W})}T^*A_* + \eta_{TG}f\omega'(G_*)\vartheta(T_*)T_*^2 - \vartheta'(T_*)A_*f\omega(G_*)T_*}, \end{array} \right. \quad (10)$$

where,

$$\left\{ \begin{array}{l} A_* = 2\frac{g_G(\mathbf{W})}{K_G(\mathbf{W})}G^* + \eta_{TG}T_*, \\ B_* = 2\frac{g_T(\mathbf{W})}{K_T(\mathbf{W})}T^* + f\omega(G_*)\vartheta(T_*). \end{array} \right. \quad (11)$$

Concerning the stability of the savanna equilibrium, the following theorem holds:

Theorem 3.3 (*Stability of the savanna equilibrium*)

The savanna equilibrium $\mathbf{E}_S = (G_*, T_*)$ is locally asymptotically stable if and only if $\mathcal{R}_*^1 < 1$ and $\mathcal{R}_*^2 > 1$.

Proof: See appendix B, page 30.

Remark 3.2 *Ecological meaning of some thresholds of model (3) are given below:*

- (i) $\mathcal{R}_{\mathbf{W}}^1 = \frac{g_T(\mathbf{W})}{\delta_T}$: is the primary production of tree biomass relative to tree biomass loss by herbivory (browsing) or human action.
- (ii) $\mathcal{R}_{\mathbf{W}}^2 = \frac{g_G(\mathbf{W})}{\delta_G + \lambda_{fG}f}$: represents the primary production of grass biomass relative to fire-induced biomass loss and additional loss due to herbivory (grazing) or human action.
- (iii) $\mathcal{R}_F = \frac{g_G(\mathbf{W})}{\eta_{TG}T^* + \delta_G + \lambda_{fG}f}$: denotes the primary production of grass biomass, relative to fire-induced grass biomass loss and additional loss due to tree/grass interactions and to herbivory (grazing) or human action at the close forest equilibrium.
- (iv) $\mathcal{R}_G = \frac{g_T(\mathbf{W})}{\delta_T + \lambda_{fT}^{max}f\omega(G^*)}$: is the primary production of tree biomass relative to fire-induced biomass loss at the grassland equilibrium and additional loss due to herbivory (browsing) or human action.

The long-term behavior of system (3) is summarized in Table 2. The dynamic can change according to the previous thresholds.

Table 2: Long term dynamic of the deterministic system (3)

$\mathcal{R}_{\mathbf{W}}^1$ ($\mathcal{R}_{\mathbf{W}}^2$)	Thresholds				Stable	Unstable	Case
	\mathcal{R}_G	\mathcal{R}_F	\mathcal{R}_*^1	\mathcal{R}_*^2			
$< 1 (< 1)$	ND	ND	NN	NN	\mathbf{E}_0		I
$> 1 (> 1)$	> 1	< 1			\mathbf{E}_F	$\mathbf{E}_0, \mathbf{E}_G$	II
	< 1	> 1	< 1	< 1	\mathbf{E}_G	$\mathbf{E}_0, \mathbf{E}_F$	III
	< 1	< 1			$\mathbf{E}_G, \mathbf{E}_F$	\mathbf{E}_0	IV
	> 1	< 1			$\mathbf{E}_F, \mathbf{E}_S$	$\mathbf{E}_0, \mathbf{E}_G$	V
	< 1	> 1	< 1	> 1	$\mathbf{E}_G, \mathbf{E}_S$	$\mathbf{E}_0, \mathbf{E}_F$	VI
	> 1	> 1			\mathbf{E}_S	$\mathbf{E}_0, \mathbf{E}_G, \mathbf{E}_F$	VII
	< 1	< 1			$\mathbf{E}_F, \mathbf{E}_S, \mathbf{E}_G$	\mathbf{E}_0	VIII

In Tables 2 and 3, the notation 'ND' stands for undefined and 'NN' denotes not necessary. It means that the threshold may take any value.

3.2 The IDE model

According to the theory of impulsive differential equation (e.g. Bainov and Simeonov, 1995, Theorem 1.1, page 3), system (4)-(5) has a unique positive solution. It is straightforward to show that the compact subset Γ is positively invariant and attracting by (4). It guarantees that model (4) is well-posed mathematically and ecologically realistic.

Providing $g_G(\mathbf{W}) = \gamma_G$, $g_T(\mathbf{W}) = \gamma_T$, $K_G(\mathbf{W}) = K_G$ and $K_T(\mathbf{W}) = K_T$, the system (4) is similar to the model developed and studied in Tchuinté Tamen et al., 2017. Thus, the demonstrations of results are the same and therefore are omitted here. Below some qualitative results of system (4) are given. There are two constant equilibria and two periodic solutions. As in subsection 3.1, the desert equilibrium $\mathbf{E}_0 = (0, 0)$ always exists and there is a forest equilibrium $\mathbf{E}_F = (0, T^*)$, when $\mathcal{R}_{\mathbf{W}}^1 > 1$, where

$$T^* = K_T(\mathbf{W}) \left(1 - \frac{1}{\mathcal{R}_{\mathbf{W}}^1} \right), \quad (12)$$

$$\mathcal{R}_{\mathbf{W}}^1 = \frac{g_T(\mathbf{W})}{\delta_T}, \quad (13)$$

and $g_T(\mathbf{W}) = \frac{\gamma_T \mathbf{W}}{b_T + \mathbf{W}}$.

Concerning the existence of the periodic grassland solution, let us set:

$$\mathcal{R}_{0,pulse}^{\bar{G}} = \frac{r_G(\mathbf{W})}{\frac{1}{\tau} \ln \left(\frac{1}{1 - \lambda_{fG}} \right)}, \quad (14)$$

and

$$\bar{G}_{per}(t) = \frac{\bar{G}(\mathbf{W})[(1 - \lambda_{fG})e^{r_G(\mathbf{W})\tau} - 1]e^{r_G(\mathbf{W})(t-n\tau)}}{[(1 - \lambda_{fG})e^{r_G(\mathbf{W})\tau} - 1]e^{r_G(\mathbf{W})(t-n\tau)} + \lambda_{fG}e^{r_G(\mathbf{W})\tau}}, \quad t \in [n\tau, (n+1)\tau[, \quad n = 0, 1, 2, \dots, \quad (15)$$

$$\text{where, } \bar{G}(\mathbf{W}) = \left(1 - \frac{1}{\bar{\mathcal{R}}_{\mathbf{W}}^2}\right) K_G(\mathbf{W}),$$

$$\bar{\mathcal{R}}_{\mathbf{W}}^2 = \frac{g_G(\mathbf{W})}{\delta_G}, \quad (16)$$

$$g_G(\mathbf{W}) = \frac{\gamma_G \mathbf{W}}{b_G + \mathbf{W}} \text{ and } r_G(\mathbf{W}) = \left(1 - \frac{1}{\bar{\mathcal{R}}_{\mathbf{W}}^2}\right) g_G(\mathbf{W}).$$

The following theorem holds:

Theorem 3.4 (*Existence of the periodic grassland solution*)

When $\mathcal{R}_{0,pulse}^{\bar{G}} > 1$, system (4) has a periodic grassland solution $\mathbf{E}_{G,per} = (\bar{G}_{per}(t), 0)$, where $\mathcal{R}_{0,pulse}^{\bar{G}}$ and $\bar{G}_{per}(t)$ are given by (14) and (15) respectively.

Proof: The proof of Theorem 3.4 is similar to the proof of Theorem 3.1 given in Tchuinté Tamen et al., 2016 (see Appendix B, page 18).

By employing the continuation theorem of the coincidence degree theory (Gaines and Mawhin, 1977, p 40), one can establish the existence of at least one positive periodic savanna solution of system (4). Set

$$\mathcal{R}_{\lambda_{fT}^*}^{*max} = \frac{r_T(\mathbf{W})}{\frac{1}{\tau} \ln \left(\frac{1}{1 - \lambda_{fT}^{*max} \omega(G_s^*)} \right)}, \quad (17)$$

and

$$\mathcal{R}_{\lambda_{fT}^{**}}^{**max} = \frac{r_T(\mathbf{W})}{\frac{1}{\tau} \ln \left(\frac{1}{1 - \lambda_{fT}^{*max} \vartheta(T_s^*) \omega(G_s^*)} \right)}, \quad (18)$$

where, $r_T(\mathbf{W}) = \left(1 - \frac{1}{\mathcal{R}_{\mathbf{W}}^1}\right) g_T(\mathbf{W})$, and

$$G_s^* = \left(1 - \frac{\delta_G}{g_G(\mathbf{W})}\right) \left(1 - \frac{1}{\mathcal{R}_{0,pulse}^{\bar{G}}}\right) K_G(\mathbf{W}), \quad (19)$$

where $\mathcal{R}_{0,pulse}^{\bar{G}}$ is given by (14) and T_s^* is the positive solution of (20)

$$(g_T(\mathbf{W}) - \delta_T) - \frac{g_T(\mathbf{W})}{K_T(\mathbf{W})} T_s^* + \frac{1}{\tau} \ln(1 - \vartheta(T_s^*) \omega(G_s^*)) = 0. \quad (20)$$

Similarly as in Tchuinté Tamen et al., 2017 (see Theorem 3.2, p 270), we claim the following result.

Theorem 3.5 (*Existence of a periodic savanna solution*). Set the following conditions:

(C1) $\mathcal{R}_{0,pulse}^{\bar{G}} > 1$ (similar as in Tchuinté Tamen et al., 2016; Tchuinté Tamen et al., 2017),

(C2) $\mathcal{R}_{\lambda_{fT}^*}^* > 1$,

(C3) $\mathcal{R}_{\lambda_{fT}^{**}}^{**} > 1$.

If (C1), (C2) and (C3) hold, then system (4) has at least one positive periodic savanna solution $\mathbf{E}_{S,per} = (G_{per}^*(t), T_{per}^*(t))$.

Proof: Proof is entirely similar as the proof of Theorem 3.2 in Tchuinté Tamen et al., 2017 (see Appendix A, p 281) and is thus omitted.

We will now examine the stability of the constant equilibria and the periodic solutions of (4). Set

$$\mathcal{R}_{0,pulse}^{\bar{G}} = \frac{g_G(\mathbf{W}) \left(1 - \frac{1}{\bar{\mathcal{R}}_{\mathbf{W}}^2}\right)}{\frac{1}{\tau} \ln \left(\frac{1}{1 - \lambda_{fG}}\right)}, \quad (21)$$

$$\bar{\mathcal{R}}_F = \frac{g_G(\mathbf{W})}{\eta_{TG}T^* + \delta_G}, \quad (22)$$

and

$$\mathcal{R}_{0,pulse}^F = \frac{g_G(\mathbf{W}) \left(1 - \frac{1}{\bar{\mathcal{R}}_F}\right)}{\frac{1}{\tau} \ln \left(\frac{1}{1 - \lambda_{fG}}\right)}, \quad (23)$$

where T^* and $\bar{\mathcal{R}}_{\mathbf{W}}^2$ are given by (12) and (16) respectively.

Concerning the stability of constant equilibria, we show Theorems 3.6 and 3.7.

Theorem 3.6 (*Stability of the desert equilibrium*).

(i) If $\mathcal{R}_{\mathbf{W}}^1 < 1$ and $\bar{\mathcal{R}}_{\mathbf{W}}^2 < 1$, then the desert equilibrium $\mathbf{E}_0 = (0, 0)$ is locally asymptotically stable (LAS).

(ii) If $\mathcal{R}_{\mathbf{W}}^1 > 1$ or $\mathcal{R}_{0,pulse}^{\bar{G}} > 1$, then the desert equilibrium is unstable.

(iii) If $\mathcal{R}_{\mathbf{W}}^1 < 1$, $\bar{\mathcal{R}}_{\mathbf{W}}^2 > 1$, and $\mathcal{R}_{0,pulse}^{\bar{G}} < 1$, then the desert equilibrium is LAS.

Theorem 3.7 (*Stability of the forest equilibrium*).

(i) If $\mathcal{R}_{\mathbf{W}}^1 < 1$, then the forest equilibrium $\mathbf{E}_F = (0, T^*)$ is unstable.

(ii) If $\mathcal{R}_{\mathbf{W}}^1 > 1$ and $\bar{\mathcal{R}}_F < 1$, then \mathbf{E}_F is LAS.

(iii) If $\mathcal{R}_{\mathbf{W}}^1 > 1$, $\bar{\mathcal{R}}_F > 1$, and $\mathcal{R}_{0,pulse}^F < 1$, then \mathbf{E}_F is LAS.

(iv) If $\mathcal{R}_{\mathbf{W}}^1 > 1$, $\bar{\mathcal{R}}_F > 1$, and $\mathcal{R}_{0,pulse}^F > 1$, then \mathbf{E}_F is unstable.

Proof: The proofs of Theorems 3.6 and 3.7 are similar to the proof of Theorem 3.3 given in Tchuinté Tamen et al., 2017 (see Appendix B, page 25).

The local stability of the periodic solutions are obtained by computing the Floquet multipliers of the monodromy matrix of (4). Set $(G_{per}(t), T_{per}(t))$ a periodic solution of (4). Consider the behaviors of small perturbations of solutions $u(t) = G(t) - G_{per}(t)$ and $v(t) = T(t) - T_{per}(t)$. The linearized system is given by:

$$\begin{pmatrix} u(t) \\ v(t) \end{pmatrix} = \Phi(t) \begin{pmatrix} u(0) \\ v(0) \end{pmatrix}, \quad (24)$$

where $\Phi(t)$ is a fundamental matrix which satisfies

$$\begin{cases} \frac{d\Phi(t)}{dt} = \begin{pmatrix} \mathcal{A}_{11}(t) & \mathcal{A}_{12}(t) \\ \mathcal{A}_{21}(t) & \mathcal{A}_{22}(t) \end{pmatrix} \Phi(t), \\ \Phi(0) = I_2, \end{cases} \quad (25)$$

where, I_2 is the identity matrix of $\mathcal{M}_2(\mathbf{R})$,

$$\begin{cases} \mathcal{A}_{11}(t) = g_G(\mathbf{W}) \left(1 - \frac{1}{\bar{\mathcal{R}}_{\mathbf{W}}^2}\right) - \frac{2g_G(\mathbf{W})}{K_G(\mathbf{W})} G_{per}(t) - \eta_{TG} T_{per}(t), \\ \mathcal{A}_{21}(t) = 0, \\ \mathcal{A}_{12}(t) = -\eta_{TG} G_{per}(t), \\ \mathcal{A}_{22}(t) = g_T(\mathbf{W}) \left(1 - \frac{1}{\mathcal{R}_{\mathbf{W}}^1}\right) - \frac{2g_T(\mathbf{W})}{K_T(\mathbf{W})} T_{per}(t). \end{cases} \quad (26)$$

Concerning the stability of the periodic grassland and the periodic savanna solutions, let us set

$$\mathcal{R}_{0,pulse}^{\bar{G}_{per}} = \frac{g_T(\mathbf{W}) \left(1 - \frac{1}{\mathcal{R}_{\mathbf{W}}^1}\right)}{\frac{1}{\tau} \ln \left(\frac{1}{1 - \lambda_{fT}^{max} \omega(\bar{G}_{per}(\tau))} \right)}, \quad (27)$$

$$\mathcal{R}_{S,pulse}^* = \frac{1}{\bar{\mathcal{R}}_{0,pulse}^{\bar{G}}} + \frac{2}{\bar{G}(\mathbf{W})} \left(\frac{1}{\tau} \int_0^\tau G_{per}^*(s) ds \right) + \frac{1}{\mathcal{R}_S^*} \left(\frac{1}{\tau} \int_0^\tau T_{per}^*(s) ds \right), \quad (28)$$

and

$$\mathcal{R}_{S,pulse}^{**} = \frac{1}{\mathcal{R}_{0,stable}^{\partial\omega}} + \frac{2}{T^*} \left(\frac{1}{\tau} \int_0^\tau T_{per}^*(s) ds \right), \quad (29)$$

where, $\bar{G}_{per}(\tau)$ is the grass biomass at the periodic grassland solution when $t = \tau$ (see (15)),

$$\bar{\mathcal{R}}_{0,pulse}^{\bar{G}} \text{ is given by (21), } \bar{G}(\mathbf{W}) = \left(1 - \frac{1}{\bar{\mathcal{R}}_{\mathbf{W}}^2}\right) K_G(\mathbf{W}), T^* = K_T(\mathbf{W}) \left(1 - \frac{1}{\mathcal{R}_{\mathbf{W}}^1}\right), \mathcal{R}_S^* = \frac{g_G(\mathbf{W}) \left(1 - \frac{1}{\bar{\mathcal{R}}_{\mathbf{W}}^2}\right)}{\eta_{TG}},$$

and $\mathcal{R}_{0,stable}^{\vartheta\omega} = \frac{g_T(\mathbf{W}) \left(1 - \frac{1}{\mathcal{R}_{\mathbf{W}}^1}\right)}{\frac{1}{\tau} \ln \left(\frac{1}{1 - \vartheta(T_{per}^*(\tau))\omega(G_{per}^*(\tau))}\right)}$, where $G_{per}^*(\tau)$ and $T_{per}^*(\tau)$ are grass biomass and tree biomass at the periodic savanna solution when $t = \tau$.

We show the following results.

Theorem 3.8 (*Stability of the periodic grassland solution*).

- (i) If $\mathcal{R}_{0,pulse}^{\bar{G}} > 1$ and $\mathcal{R}_{0,pulse}^{\bar{G}_{per}} < 1$, then the periodic grassland solution $\mathbf{E}_{G,per} = (\bar{G}_{per}(t), 0)$ is LAS.
- (ii) If $\mathcal{R}_{0,pulse}^{\bar{G}} > 1$ and $\mathcal{R}_{0,pulse}^{\bar{G}_{per}} > 1$, then the periodic grassland solution is unstable.

Proof: The proof of Theorem 3.8 is similar to the proof of Theorem 3.4 given in Tchuinté Tamen et al., 2017 (see Appendix C, page 26).

Theorem 3.9 (*Stability of the periodic savanna solution*).

- (i) If $\mathcal{R}_{S,pulse}^* > 1$ and $\mathcal{R}_{S,pulse}^{**} > 1$, then the periodic savanna solution $\mathbf{E}_{S,per} = (G_{per}^*(t), T_{per}^*(t))$ is LAS.
- (ii) If $\mathcal{R}_{S,pulse}^* < 1$ or $\mathcal{R}_{S,pulse}^{**} < 1$, then $\mathbf{E}_{S,per}$ is unstable.

Proof: The proof of Theorem 3.9 is similar to the proof of Theorem 3.5 given in Tchuinté Tamen et al., 2017 (see Appendix D, page 27).

Based on the previous results, we summarize the long-term behaviors of system (4) in Table 3.

Table 3: Long term dynamic of the semi-discrete system (4)

		Thresholds					Stable	Unstable	Case
$\mathcal{R}_{\mathbf{W}}^1$ ($\bar{\mathcal{R}}_{\mathbf{W}}^2$)	$\mathcal{R}_{0,pulse}^{\bar{G}}$	$\bar{\mathcal{R}}_F$	$\mathcal{R}_{0,pulse}^F$	$\mathcal{R}_{0,pulse}^{G_{per}}$	$\mathcal{R}_{S,pulse}^*$	$\mathcal{R}_{S,pulse}^{**}$			
< 1 (NN)	< 1	ND	ND	NN	NN	NN	\mathbf{E}_0		I
		< 1	NN	> 1			\mathbf{E}_F	$\mathbf{E}_0, \mathbf{E}_{G,per}$ $\mathbf{E}_{S,per}$	II
			> 1	< 1	< 1	< 1	$\mathbf{E}_{G,per}$	$\mathbf{E}_0, \mathbf{E}_F$ $\mathbf{E}_{S,per}$	III
		> 1					$\mathbf{E}_F, \mathbf{E}_{G,per}$	$\mathbf{E}_0, \mathbf{E}_{S,per}$	IV
> 1 (> 1)	> 1		< 1	> 1			$\mathbf{E}_F, \mathbf{E}_{S,per}$	$\mathbf{E}_0, \mathbf{E}_{G,per}$	V
				< 1			$\mathbf{E}_F, \mathbf{E}_{S,per}, \mathbf{E}_{G,per}$	\mathbf{E}_0	VI
					> 1	> 1	$\mathbf{E}_{G,per}, \mathbf{E}_{S,per}$	$\mathbf{E}_0, \mathbf{E}_F$	VII
		< 1	> 1	> 1			$\mathbf{E}_{S,per}$	$\mathbf{E}_0, \mathbf{E}_F$ $\mathbf{E}_{G,per}$	VIII

4 Numerical simulations and discussion

Like in our previous works (Tchuinté Tamen et al., 2014; Tchuinté Tamen et al., 2017) we use the nonstandard finite difference (NSFD) scheme to solve systems (3) and (4) numerically and provide simulations that strictly comply with the properties of the systems. The nonstandard approach has shown to be very effective to solve dynamical systems in biosciences (see for instance Anguelov et al., 2012 and references therein). Parameter values used for numerical simulations are given in Table 4.

Table 4: Parameter values related to Fig. 3-(b) and Figs. 4–11. .

$c_G, \text{t.ha}^{-1}$	$c_T, \text{t.ha}^{-1}$	$b_G, \text{mm.yr}^{-1}$	$b_T, \text{mm.yr}^{-1}$	a_G, yr^{-1}	a_T, yr^{-1}
20	450	501	1192	0.0029	0.0045
$d_G, -$	$d_T, -$	γ_G, yr^{-1}	γ_T, yr^{-1}	δ_G, yr^{-1}	δ_T, yr^{-1}
14.73	106.7	2.5	1	0.01	0.1
$\lambda_{fG}, -$	$\lambda_{fT}^{\min}, -$	$\lambda_{fT}^{\max}, -$	$p, \text{t}^{-1}\text{ha}$	$\alpha, \text{t.ha}^{-1}$	$\eta_{TG}, \text{ha.t}^{-1}\text{yr}^{-1}$
0.3	0.05	0.7	0.01	1	0.01

4.1 Bifurcation map

A bifurcation is a qualitative change of the behaviors of the system when some parameters cross particular values. Following Accatino et al., 2010, we use a graphical Matlab toolbox (MATLAB) called Matcont to build the bifurcation diagrams of our model. Matcont is a useful software which allows computing numerical continuation of equilibria, limit points, Hopf points, branch points of equilibria, limit cycles, fold, flip, torus and branch point bifurcation points of limit cycles, and homoclinic orbits of dynamical systems. It is freely available online according to <http://www.matcont.ugent.be/>. One can use Matcont to compute a codimension 1 (i.e., one control parameter) or codimension 2 bifurcations. Here, we perform a bifurcation diagram of codimension 2 in the environmental space defined by the mean annual precipitation (MAP) \mathbf{W} and fire frequency f (see Fig. 3). The readers can refer to Dhooge et al., 2003; Dhooge et al., 2006; Govaerts et al., 2007 and references therein for more details and examples on numerical methods for two-parameter bifurcation analysis in Matcont. See Appendix C, page 32 for a condensed overview of explanations of how model (3) is implemented into MatCont.

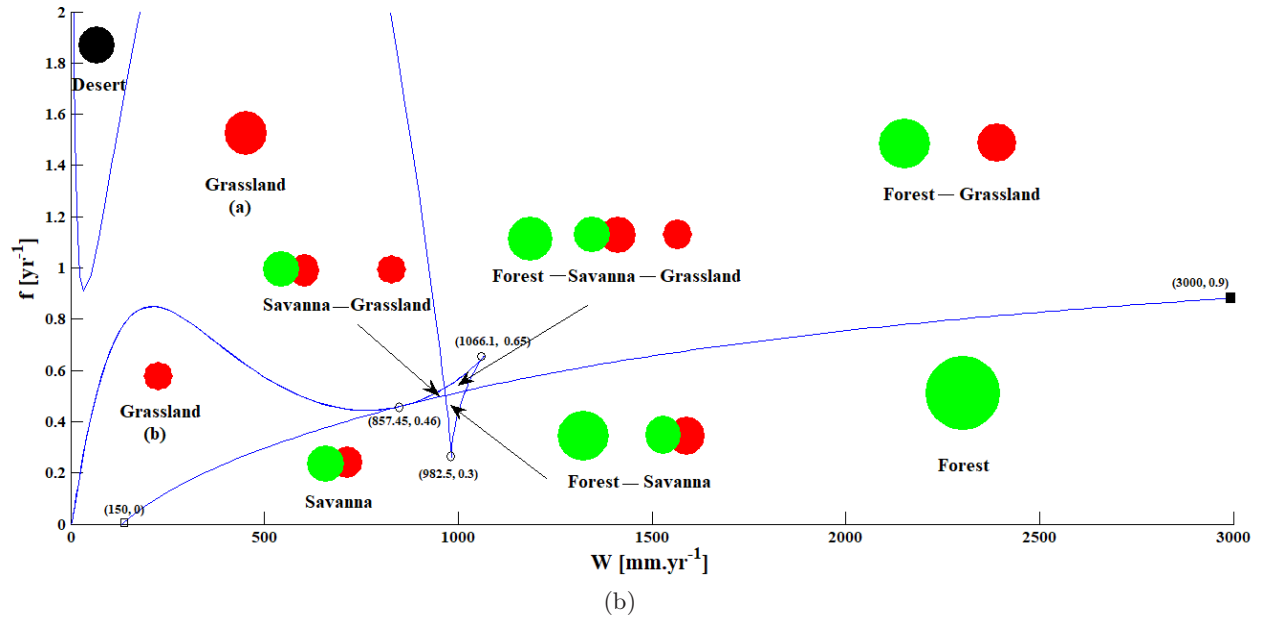
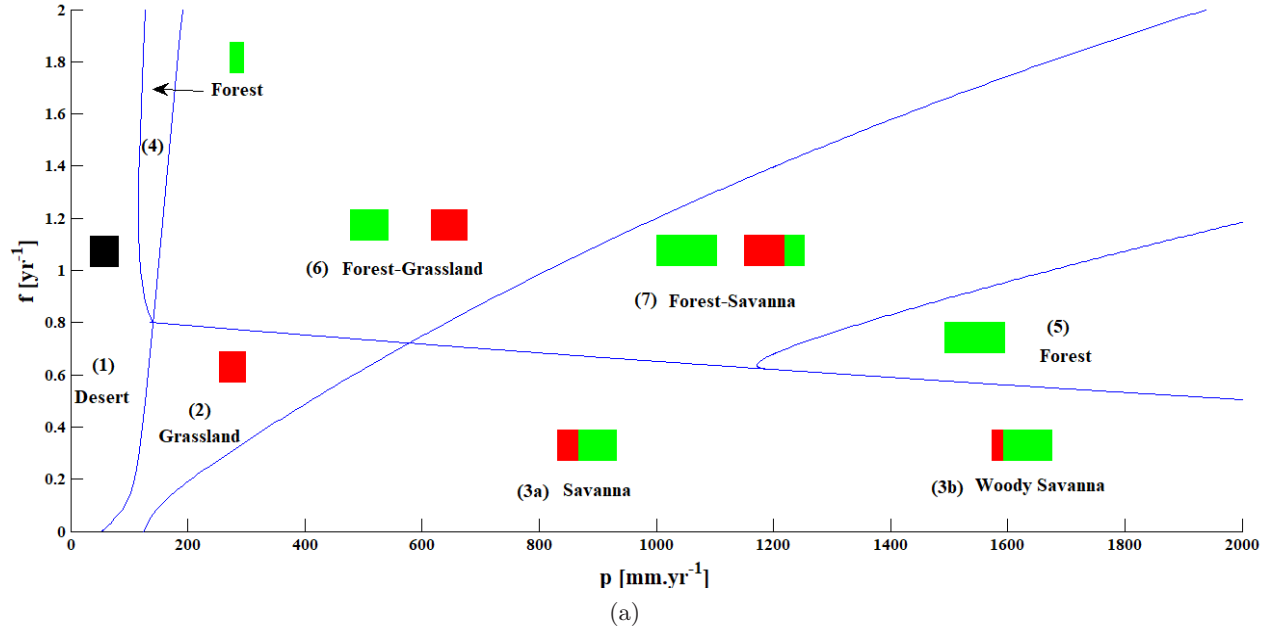


Figure 3: Bifurcation diagrams using Matcont. (a) reproduces the diagram of the Accatino et al., 2010 model (see figure 2 in Accatino et al., 2010 for parameter values used). (b) is the diagram of system (3). Single red, green and black rectangles in panel (a) (dots in panel (b)) stand for grassland, forest and desert respectively. Twinned red and green symbols stand for savanna (coexistence state). Size of the symbols qualitatively denote grass and tree covers in panel (a) and biomass levels in panel (b). The parameter values used for Fig. 3-(b) are given in Table 2. (Color in the online version).

The bifurcation diagram of model (3) is provided in Fig. 3-(b) in the two dimensional parameter space (f vs. W) using Matcont. Depending on those parameters, the system involves both

monostable and multi-stable situations. Once a bifurcation point in the parameter space (see e.g., cusp points represented by circles) is found, Matcont produces the entire bifurcation curve passing through that point. Blue curves which partition the parameter space into subregions are bifurcation curves. Trajectories starting in the same subregion have qualitatively the same dynamics. It is also important to note that when the mean annual precipitation (MAP) increases, we logically observe a gradual increase of tree biomass for any given level of f . For instance in Fig. 3-(b), considering low values of f (say < 0.3) the savanna cede pace to forest as W increases. On the other hand, several scenarios are possible when the fire frequency increases depending on the range of W values. Fig. 3-(a) shows the complete dynamics of the Accatino et al., 2010 model and Fig. 3-(b) shows the complete long term dynamics of system (3) in specified (rainfall, fire frequency) parameter ranges. There are two main observations: (i) Fig. 3-(b) shows a bistability between grassland and savanna (see also Fig. 4-(b) for an illustration) and a tristability between forest, savanna and grassland (see also Fig. 5-(a)) while these subregions do not exist in Fig. 3-(a); (ii) in Fig. 3-(a), when fire frequency decreases the system does not favor tree expansion whatever the context (semi-arid, mesic and humid), while an opposite trend is observed in Fig. 3-(b). For instance in Fig. 3-(a) between ca. 600–1200 mm.yr⁻¹ the Accatino et al., 2010 system can shift from a bistability between forest and savanna (see the subregion (7)) to a monostability of savanna (see the subregion (3a)). Moreover above ca. 1200 mm.yr⁻¹ their system can shift from forest (see the subregion (5)) to savanna woodland (see the subregion (3b)). On the contrary, in Fig. 3-(b), decreasing the fire frequency favors the tree expansion whatever the climatic context. This is in agreement with what is observed in the field as suggested by several empirical studies (Mitchard et al., 2009; Bond and Parr, 2010; Favier et al., 2012; Mitchard and Flintrop, 2013 for a review). For instance in Fig. 3-(b), between ca. 600 – 1200 mm.yr⁻¹ model (3) predicts three scenarios: In scenario 1 the system can shift from grassland to savanna, in scenario 2 the system can shift from grassland to monostability of a savanna woodland passing through a bistability between grassland and savanna (see also Fig. 4 for trajectories illustrating this transition). In scenario 3, the system can shift from a bistability between forest and grassland to forest passing through a tristability between forest, savanna and grassland and a bistability between forest and savanna (see also Fig. 5 for an illustration of this transition). Above ca. 1200 mm.yr⁻¹ the system can shift from a bistability between forest and grassland to a monostability of forest.

4.2 Illustrations and discussion

Throughout this subsection, the simulations provided with our minimalistic ODE model (3) and IDE model (4) show the well-known fact that increasing fire return period systematically implies an increase in woody biomass. This is pivotal when one describes the tree-grass dynamics in fire-prone savanna ecosystems (Bond et al., 2005; Bond and Parr, 2010; Mitchard and Flintrop (2013)). As far as we know, it is a completely new feature for 'minimalistic' tree-grass ODE models, that has not been reported in previous models with only two state variables.

Though the model aims to be qualitatively relevant for a large swath of African situation, we ground our simulations in a selected north-south gradient located at the 16 °E of longitude, and between ca. 6 and 10 °N of latitude (i.e., between ca. 900 to 1500 mm.yr⁻¹ of MAP). The area goes from the Adamawa region to the Centre region in Cameroon and it spans the main vegetation physiognomies of Central Africa. Using longitude and latitude data, the MAP data were extracted from BIO12 (<http://www.worldclim.org/bioclim>, see also Hijmans et al., 2005) using the "raster"

package of RStudio, version 1.1.383.

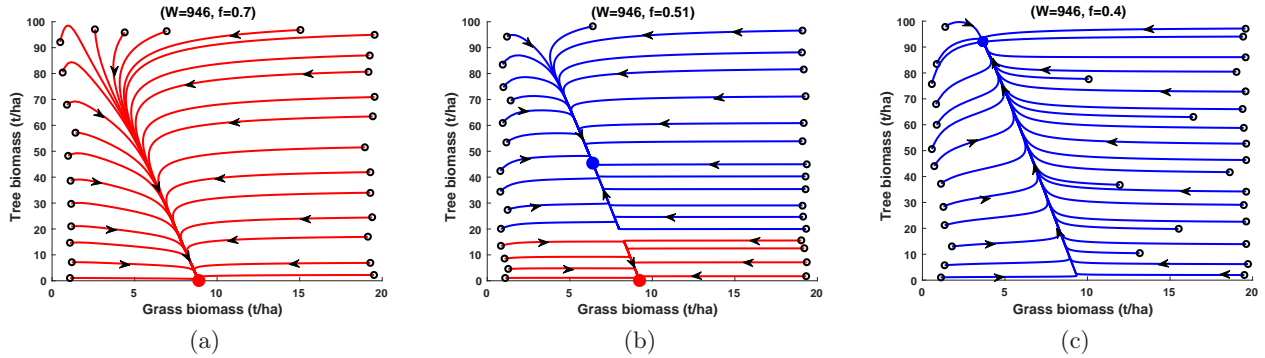


Figure 4: Illustration of a bifurcation due to the fire frequency f with the continuous model (3). Here, $\mathbf{W} = 946 \text{ mm.yr}^{-1}$. Open black circles are initial conditions. Blue and red dots are savanna and grassland equilibria respectively. (Color in the online version).

In Fig. 4, a decrease in the fire frequency f from 0.7 to 0.51, then to 0.4, leads the ODE system to shift from grassland state to a savanna-grassland bistable state, and then to a savanna woodland state under a constant \mathbf{W} (MAP) of ca. 950 mm.yr^{-1} .

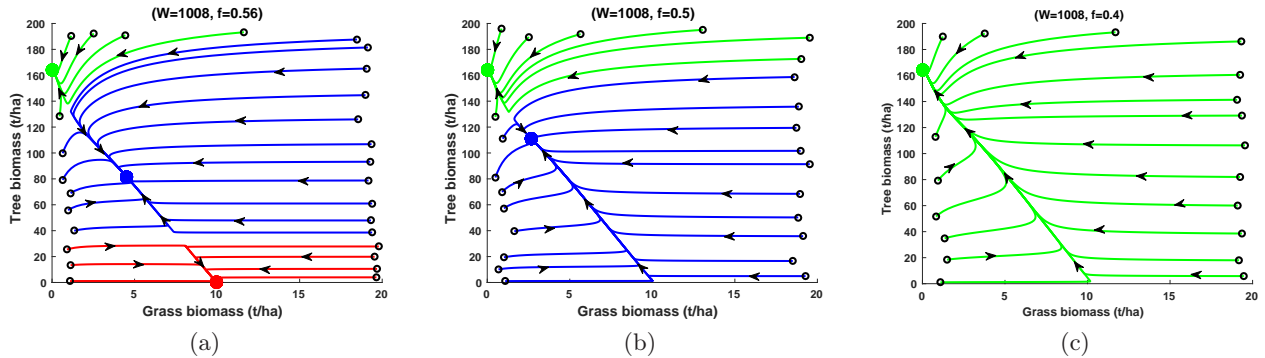


Figure 5: Bifurcation due to the fire frequency f with the continuous model (3) for rainfall slightly above 1008 mm.yr^{-1} .

Fig. 5 illustrates a bifurcation from a forest-savanna-grassland tristable state to a forest state passing through a forest-savanna bistable state, for a constant MAP \mathbf{W} of ca. 1000 mm.yr^{-1} under a decrease of fire frequency f . Domains of stability for grassland, savanna and forest are in red, blue and green, respectively. Forest expansion has been regularly observed at local and regional scales when the fire frequency decreases (see Mitchard and Flintrop, 2013 for a review).

With the MAP values chosen for Fig. 4 and Fig. 5, we aimed to document the critical parameter space area where the multi-stability between the main vegetation physiognomies occur. It is indeed a stretch of the rainfall gradient where notable differences in biomasses are observed in relation to variations in fire frequencies (see Fig. 6).

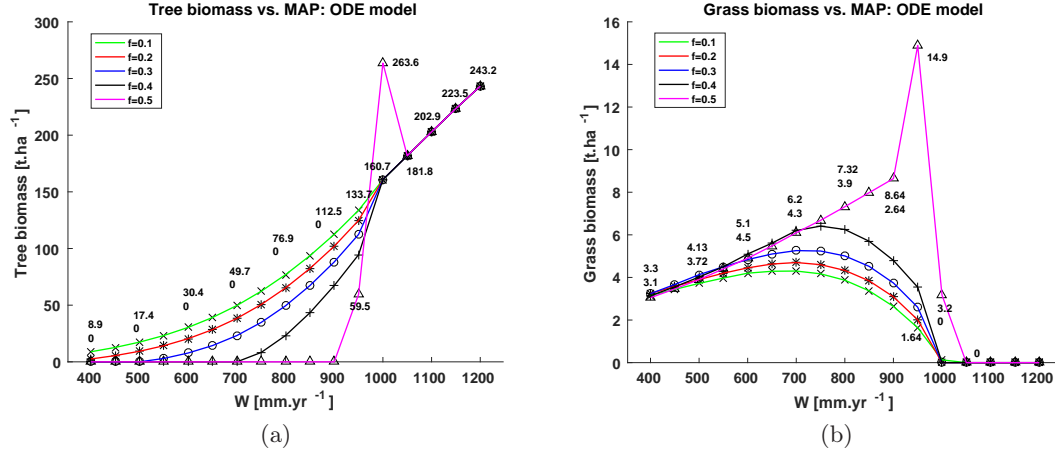


Figure 6: Expected tree (a) and grass (b) biomasses as functions of MAP (\mathbf{W}) and fire frequencies (f , yr^{-1}) with the ODE model. Expected maximum and minimum biomass values are mentioned for a set of \mathbf{W} values used in simulations. The peak values of the magenta curves in panels (a) and (b) are the expected biomasses at the forest-savanna bistable state and savanna-grassland bistable state respectively. (Color in the online version).

Fig. 6 illustrates the expected tree and grass biomasses (at the equilibrium) versus rainfall for $f = 0.1, 0.2, 0.3, 0.4$ and 0.5 fires per year. It is related to Fig. 7-(a) and it shows a progressive increase of the tree biomass and a decrease of the grass biomass when the mean annual precipitation (MAP) \mathbf{W} increases.

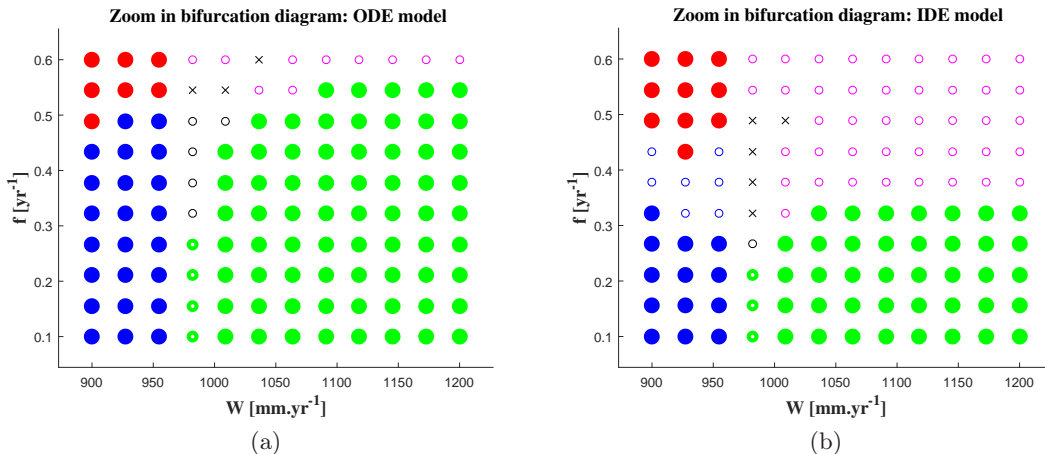


Figure 7: Zoom in the outcomes of models (3) and (4) evaluated along gradients of MAP (\mathbf{W}) and fire frequency f . The red, blue and green dots stand for grassland, savanna and forest respectively. The magenta and blue circles stand for bistability between forest and grassland, and bistability between savanna and grassland respectively. The black and green circles stand for bistability between forest and savanna; and monostability of the woody savanna respectively. The symbol of the cross denotes the tristability situation. (Color in the online version).

Fig. 7 shows the model outputs for system (4) depending on fire frequency and mean annual

precipitation. It is an analogue pulsed version of the bifurcation diagram given in Fig. 3. Fig. 7-(a) is a zoom of the bifurcation diagram given in Fig. 3-(b) for $(f, \mathbf{W}) \in [0, 0.6] \times [900, 1200]$ and Fig. 7-(b) is the analogous IDE version of Fig. 7-(a). Indeed Figs. 7-(a) and (b) qualitatively show the same model outcomes, but it seems that the transversal bifurcation curve of Fig. 3-(b) (see the blue line linking the empty and bold squares) shifts down with the IDE analogue. It means that at the same level of precipitation using the IDE model (4), bifurcations are predicted at lower fire frequencies than with the ODE model (3) (see for example Figs. 4 and 8). It implies that for a given level of precipitations preserving the forest-grassland bistability would necessitate a smaller fire frequency according to the IDE model than with the ODE model.

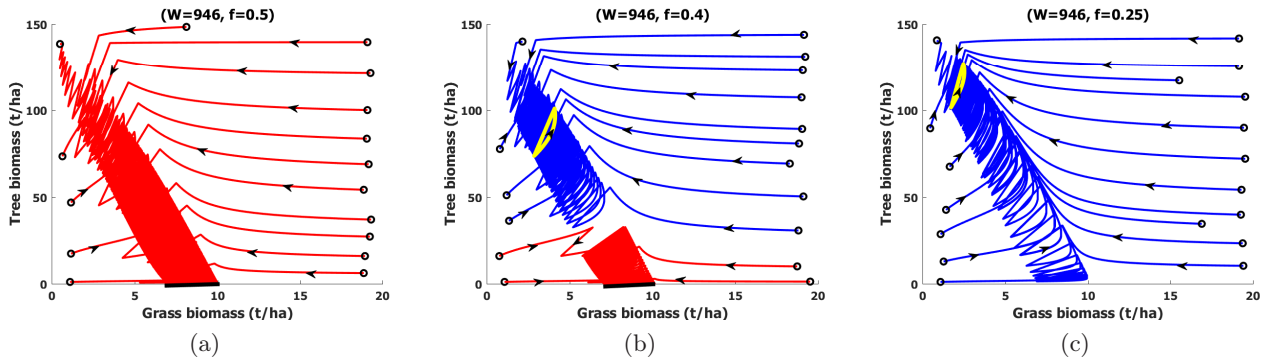


Figure 8: Illustration of a bifurcation due to fire frequency f with the impulsive model (4). Fig. 4 and this figure have same parameters with varying fire frequencies. The yellow curve and black segment denote the periodic savanna (in fact woodland) and grassland solutions respectively.

Both Figs. 8 and 4 plotted respectively for the IDE model (4) and ODE model (3) show qualitatively similar behaviors corresponding to a decrease in fire frequency for constant rainfall. In Fig. 8, when f decreases, the system shifts from a monostable periodic grassland (see panel (a)) to a monostable periodic savanna (see panel (c)) passing through a bistability between periodic savanna and periodic grassland solutions (see panel (b)).

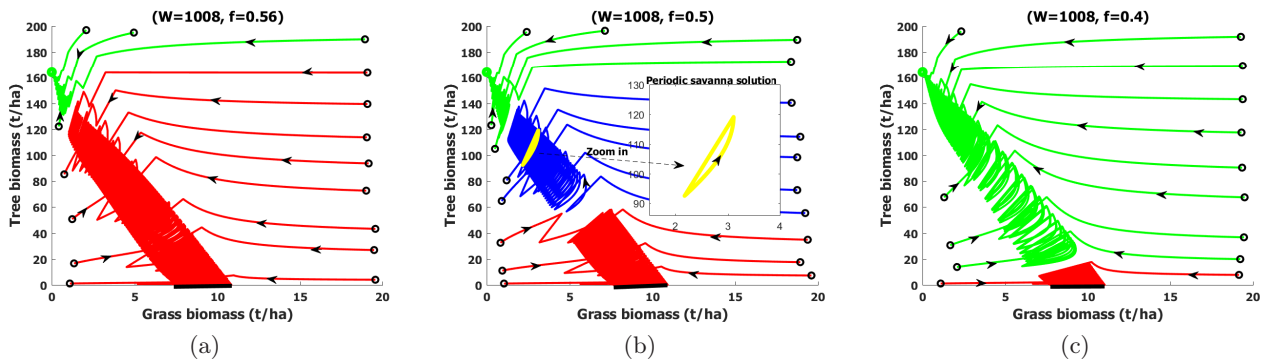


Figure 9: Illustration of a bifurcation due to a decrease in fire frequency f with the IDE model (4). Both Fig. 5 (ODE) and this figure have same MAP $\mathbf{W} = 1008 \text{ mm.yr}^{-1}$ and same sequence of f values. The yellow curve and black segment denote the periodic savanna and grassland solutions respectively.

Fig. 9 shows a bifurcation due to f using the IDE model (4). It illustrates the expansion of forest into savanna and grassland when f decreases. For $f = 0.56$, panel (a) in Fig. 9 shows a bistability associating forest and a periodic grassland (having a big basin of attraction). When f decreases from 0.56 to 0.5 the system bifurcates to a tristability between forest and two periodic solutions: savanna and grassland (see panel (b) in Fig. 9). Further decrease of f from 0.5 to 0.4 leads the system to bifurcate to a bistability associating forest and a periodic grassland solution with a small basin of attraction (see panel (c) in Fig. 9).

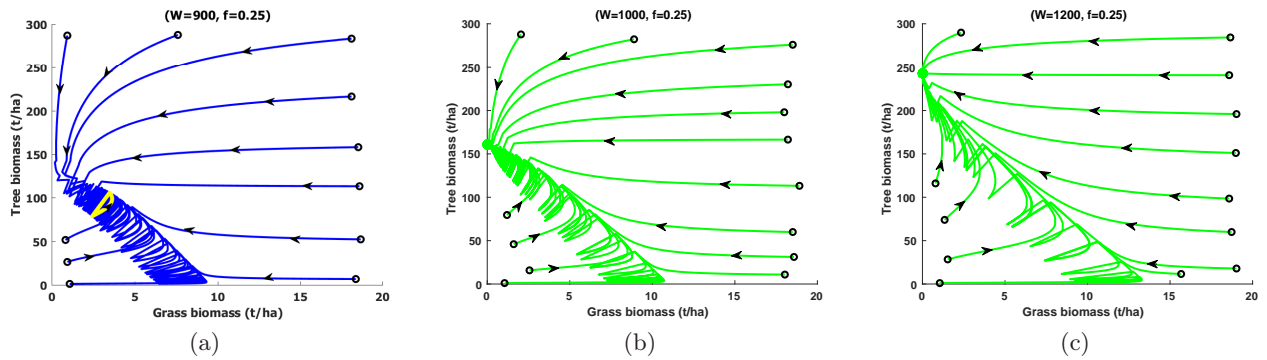


Figure 10: This figure shows a bifurcation from periodic savanna to forest with increasing MAP W for a rather low annual fire frequency value i.e., $f = 0.25$ with the IDE model (4).

Fig. 10 illustrates a bifurcation due to W using the IDE model (4). An increase of the MAP W leads the system to shift from a periodic savanna solution to a forest state under a constant fire frequency value $f = 0.25$.

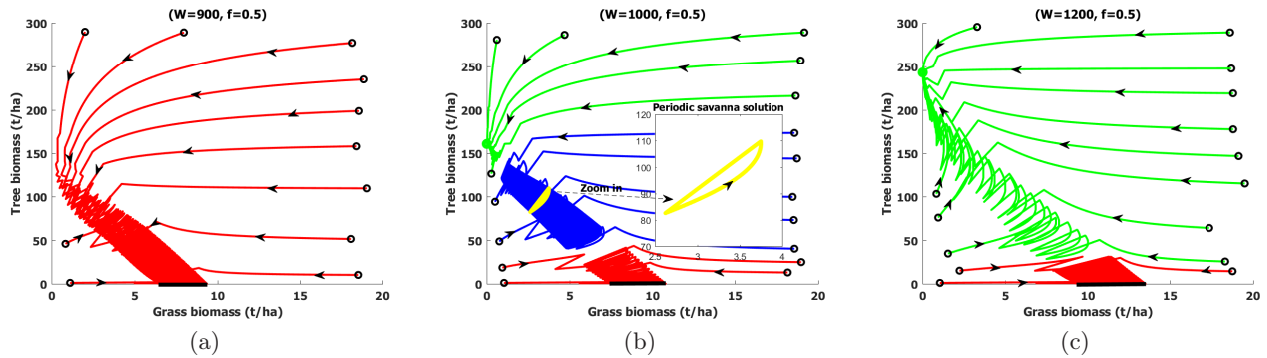


Figure 11: Illustration of a bifurcation due to an increase in the MAP W with the IDE model (4). Here $f = 0.5$.

In Fig. 11, when the MAP W increases in presence of a higher fire frequency (compared to Fig. 10), the system bifurcates from a periodic grassland solution (see panel (a)) to a bistability between forest and a periodic grassland solution (see panel (c)) passing through a tristability associating forest, periodic savanna and grassland solutions (see panel (b)).

In the literature most tree-grass dynamical systems based on differential equations were analysed focusing on the stable vegetation states, but never on the trajectories. This has been criticized

recently by Accatino and De Michele, 2016 who compared two modelling approaches of tree-grass savanna dynamics they used and that differ in several aspects, notably with respect to the way in which fire is modelled. The first modelling approach which is referred to equilibrium model (EM) considers fire occurrence as a constant parameter, whereas the second modelling approach which is referred as non-equilibrium model (NEM) considers fire occurrence as a stochastic event whose probability depends on the amount of dry grass biomass which is built-up in the preceding rainy seasons. According to Accatino and De Michele, 2016, one fundamental difference between EM and NEM resides in how their two models can be analysed. While EM analyses are focused on steady states, NEM analyses also extent to trajectories. Indeed, the Accatino and De Michele, 2016 study shows that their EM modelling has some limitations concerning predictions of woody cover variation along a rainfall gradient, while several aspects simultaneously contribute to more satisfactory results obtained with NEM. Here, we have illustrated the fact that predictions that are qualitatively satisfactory can be obtained by directly improving the ODE based 'EM' framework, notably regarding the fire induced mortality on woody biomass expressed through two independent non-linear functions $\omega(G)$ (see (1)) and $\vartheta(T)$ (see (2)). Nonlinear shape of $\omega(G)$ was also retained by some other authors (Scheiter and Higgins, 2007; Higgins et al., 2010; Staver et al., 2011b; Van Nes et al., 2014; Yu and D'Odorico, 2014) to model the fire mediated feedback of grass onto tree dynamics. The function $\vartheta(T)$ was introduced in our previous tree-grass model (Tchuinté Tamen et al. (2017)) to take into account the response of trees to fires of a given intensity. With our ODE based 'EM' framework, we illustrated how stable vegetation equilibria varied in function of MAP and fire frequency (see Fig. 7-(a)), and for five values of f : 0.1, 0.2, 0.3, 0.4 and 0.5, we also illustrated the long-term trajectories expected for tree and grass biomasses at the equilibrium for different levels along a rainfall gradient (see Fig. 6). The analysis of these trajectories would be meaningful per se.

Most savanna fires burn due to human ignition (Favier et al., 2004; Govender et al., 2006; Archibald et al., 2009), but it is believed that these systems are seldom ignition limited, and more often limited by available fuel (Archibald et al., 2010; van Leeuwen et al., 2014). Accatino and De Michele, 2016 underlined the questionable assumption according to which the parameter f of fire frequency should be independent of vegetation characteristics. According to Accatino and De Michele (2016), fire frequency should be considered an emergent property of the dynamical system. This is in contrast with many EM which consider fire as a priori determined and constant parameter. Here, in our ODE based EM framework, fire frequency f is kept as constant multiplier of $\omega(G)$ (non-linear and bounded function of grass biomass, see (1)), but we interpret it as a man-induced "targeted" fire frequency (as for instance in a fire management plan), which will not translate into actual frequency of fires of notable impact (because of $\omega(G)$ being in its low branch) as long as grass biomass is not of sufficient quantity. We thereby split fire frequency from fire impact. This modelling choice is based on the known fact that grass biomass controls fire spread (Govender et al., 2006; van Leeuwen et al., 2014). The $\omega(G)$ function is also expected to take into account the difficult spreading of fire due to fuel of average low quantity keeping in mind natural spatial variability of grass biomass. Low grassy fuel results in lower-fire intensities that barely propagate leaving a large share of the area unburnt, as frequently observed in the field (see Diouf et al., 2012). This makes the difference between: (i) fire frequency f to be seen as an external forcing upon the tree-grass system (think about a targeted fire regime in a managed area such as a ranch or a national park); and (ii) actual yearly fire probability (or frequency) of occurrence in any arbitrary piece of land when (i) has been set. Moreover, relationship between the proportion of the area burnt and grass abundance is likely to be sharply nonlinear, as suggested by the impressive results reported by McNaughton, 1992 at the

scale of the entire Serengeti National Park (Tanzania). According to McNaughton, 1992, herbivory can produce extensive firebreaks creating a landscape mosaic which drastically limits fire spreading. Local fire frequency dwindled over a decade following grass biomass suppression by soaring herbivore populations, while the ignition regime by communities dwelling around the park likely remained more or less the same (McNaughton, 1992).

Using a very simple ODE model, Staver et al., 2011b concluded that fire cannot influence vegetation but for MAP above 1000 mm.yr^{-1} . Referring to a more complicated simulation "gap" model, Lehsten et al., 2016 reached results that suggest significant fire influence from 400 mm MAP upwards. Experimental data from the Kruger National Park (Govender et al., 2006; Lehsten et al., 2016) suggest notable fire influence below 700 mm.yr^{-1} . In Fig. 6 we reach the conclusion that fire frequency considerably change the expected biomasses for MAP values under 1000 mm.yr^{-1} , while our Fig. 3 suggests that fire may be able to contribute to the savanna vs. grassland bifurcation for MAP values in the range $500 - 1000 \text{ mm.yr}^{-1}$

5 Conclusion

Here, we have developed and presented a 'minimalistic' tree-grass model that considers interactions of fire and water availability in tree-grass ecosystems. Our model integrates the mean annual precipitation (MAP) as a parameter which shapes growth rates and carrying capacities of tree and grass biomasses. It is to our best knowledge the first time that consistent responses curves (Fig. 2) are assessed from existing information all along the rainfall gradient. The ODE version of the model is fully mathematically tractable as are most of the results relating to the IDE analogue. Compared to Tchuinté Tamen et al., 2017, the novelty in the present contribution is that we combine pulsed fire and precipitation-explicit vegetation growth in order to study how the frequency of pulsed fires shapes the vegetation along the rainfall gradient. Both ODE and IDE versions differ fundamentally from existing tree-grass models in the literature in the way that water availability is considered. Some existing models considered additional soil moisture variables (e.g., Accatino et al., 2010; Yu and D'Odorico, 2014) leading to more complex set of parameters and more complex mathematical systems. But, there is no need of an additional equation about soil moisture since its dynamic is very rapid compared to change in vegetation (fast and slow variables) (Barbier et al., 2008; Martínez-García et al., 2013). According to our bifurcation diagram (see Fig. 3-(b)), we were able to account for a wide range of physiognomies and dynamical outcomes of the tree-grass system at regional-continental scales by relying on a simple model that explicitly address some essential processes that are: (i) limits put by rainfall on vegetation growth and standing biomass (ii) asymmetric interactions between woody and herbaceous plant life forms, (iii) positive feedback between grass biomass and fire intensity and decreased fire impact with tree height (in fact cumulated woody biomass in the model). For tree-grass ODE frameworks, two very general bifurcation diagrams ('big pictures') were produced to predict the vegetation dynamics in the parameters space defined by rainfall and fire frequency: Fig. 3-(a) from Accatino et al., 2010 and Fig. 3-(b) from our model (3). Fig. 3-(b) improves the results found in Fig. 3-(a) since it predicts more diverse possible situations. For instance it shows a domain where grassland and savanna are bistable and a domain where forest, savanna and grassland are tristable. These vegetation outcomes agree with results found by remotely-sensed studies (Hirota et al., 2011; Favier et al., 2012). Along a general transect over Central Africa, according to Favier et al., 2012 (Figure 2-(e)), there is a bistability associating sparsely wooded savanna and grassland at ca. 800 mm.yr^{-1} and tristability is observed very locally

around latitude of 7 – 10 °N (north) (i.e., between ca. 1031 and 1475 mm.yr⁻¹ of MAP).

Under its impulsive form, model (4) presented here is an extension of our previous IDE model where we already considered the fire induced mortality on woody biomass by mean of two independent non-linear functions, namely ω (see 1) and ϑ (see 2; Tchuinté Tamen et al., 2017; Tchuinté Tamen, 2017). In the present paper we showed that the introduction of these two functions was in fact decisive since even the ODE version of the model proved able to provide sensible results. Notably, we showed that increasing fire return period systematically leads the system to switch from grassland or savanna to forest (forest encroachment). This result is entirely consistent with field observations (Bond et al., 2005; Bond and Parr, 2010; Favier et al., 2012; Jeffery et al., 2014). But to our knowledge, it is not established that any other model with only two-state variables is able to retrieve this fundamental behavior. Some more complex models may also fail to display the right behavior in some particular ecological contexts. This should be considered as benchmarking test for existing models.

Acknowledgements A. Tchuinté Tamen gratefully acknowledges financial supports of the French Embassy in Yaoundé (Cameroon) through the SCAC fund 2015, and the French National Institute for Research for Sustainable Development (IRD) in Yaoundé (Cameroon) during the preparation of this manuscript. He thanks Prof. S. Bowong and Prof. J.J. Tewa for their helps and fruitful discussions throughout this work. He also thanks researchers of the UMR-AMAP Laboratory in Montpellier (France) for useful interactions during his internship at AMAP Lab.

Appendix A: Proof of Theorem 3.1 (Existence of a savanna equilibrium)

From system (3), a savanna equilibrium $\mathbf{E}_S = (G_*, T_*)$ satisfies

$$\begin{cases} g_G(\mathbf{W}) \left(1 - \frac{G_*}{K_G(\mathbf{W})}\right) - (\delta_G + \lambda_{fG}f) - \eta_{TG}T_* = 0, \\ g_T(\mathbf{W}) \left(1 - \frac{T_*}{K_T(\mathbf{W})}\right) - \delta_T - f\vartheta(T_*)\omega(G_*) = 0. \end{cases} \quad (30)$$

Using the first equation of (30), we have

$$T_* = \frac{1}{\eta_{TG}} \left(g_G(\mathbf{W}) - (\delta_G + \lambda_{fG}f) - \frac{g_G(\mathbf{W})}{K_G(\mathbf{W})}G_* \right) = \frac{g_G(\mathbf{W})}{\eta_{TG}K_G(\mathbf{W})}(G^* - G_*). \quad (31)$$

From (31) note that one of the conditions to have a plausible savanna equilibrium is:

$$G^* > G_*. \quad (32)$$

Substituting (31) in the second equation of (30) gives

$$\frac{(g_T(\mathbf{W}) - \delta_T) - \frac{g_G(\mathbf{W})g_T(\mathbf{W})}{\eta_{TG}K_G(\mathbf{W})K_T(\mathbf{W})}(G^* - G_*)}{\omega(G_*)} = f\vartheta(T_*). \quad (33)$$

From (33), introducing the expression of $\omega(G)$, we have

$$\frac{\frac{g_T(\mathbf{W})}{K_T(\mathbf{W})}T^* - \frac{g_G(\mathbf{W})g_T(\mathbf{W})}{\eta_{TG}K_G(\mathbf{W})K_T(\mathbf{W})}G^* + \frac{g_G(\mathbf{W})g_T(\mathbf{W})}{\eta_{TG}K_G(\mathbf{W})K_T(\mathbf{W})}G_*}{\frac{G_*^2}{G_*^2 + \alpha^2}} = f\vartheta(T_*), \quad (34)$$

where

$$f\vartheta(T_*) = f\lambda_{fT}^{min} + f(\lambda_{fT}^{max} - \lambda_{fT}^{min}) \times e^{-p \frac{g_G(\mathbf{W})G^*}{\eta_{TG}K_G(\mathbf{W})}} \times e^{p \frac{g_G(\mathbf{W})G_*}{\eta_{TG}K_G(\mathbf{W})}}. \quad (35)$$

From (34) and (35) we have:

$$(a - b + cG_*) \left(1 + \frac{\alpha^2}{G_*^2}\right) = d + \lambda e^{\alpha G_*}, \quad (36)$$

where,

$$a = \frac{g_T(\mathbf{W})}{K_T(\mathbf{W})}T^*, \quad b = \frac{g_G(\mathbf{W})g_T(\mathbf{W})}{\eta_{TG}K_G(\mathbf{W})K_T(\mathbf{W})}G^*, \quad c = \frac{b}{G_*}, \quad d = f\lambda_{fT}^{min}, \quad \lambda = f(\lambda_{fT}^{max} - \lambda_{fT}^{min}) \times e^{-p \frac{g_G(\mathbf{W})G^*}{\eta_{TG}K_G(\mathbf{W})}} \text{ and } \alpha = p \frac{g_G(\mathbf{W})}{\eta_{TG}K_G(\mathbf{W})}.$$

From equation (36) we have

$$cG_*^3 - \lambda G_*^2 e^{\alpha G_*} + (a - b - d)G_*^2 + c\alpha^2 G_* + (a - b)\alpha^2 = 0. \quad (37)$$

Set $H(G_*) = cG_*^3 - \lambda G_*^2 e^{\alpha G_*} + (a - b - d)G_*^2 + c\alpha^2 G_* + (a - b)\alpha^2$. H is a function of one variable $G_* \in]0, +\infty[$. To find the number of real positive roots of $H(G_*)$, we will use the intermediate value theorem which is generally good for investigating real roots of differentiable and monotonous functions.

We have

$$\begin{cases} \lim_{G_* \rightarrow 0} H(G_*) = (a - b)\alpha^2, \\ \lim_{G_* \rightarrow +\infty} H(G_*) = -\infty. \end{cases} \quad (38)$$

The derivative of H is $H'(G_*) = 3cG_*^2 - \lambda(\alpha G_*^2 + 2G_*)e^{\alpha G_*} + 2(a - b - d)G_* + c\alpha^2$. We have

$$\begin{cases} \lim_{G_* \rightarrow 0} H'(G_*) = c\alpha^2 > 0, \\ \lim_{G_* \rightarrow +\infty} H'(G_*) = -\infty. \end{cases} \quad (39)$$

Denote by H_1 the derivative of H' . We have $H_1(G_*) = 6cG_* - \lambda(\alpha^2 G_*^2 + 4\alpha G_* + 2)e^{\alpha G_*} + 2(a - b - d)$. The limits of $H_1(G_*)$ at 0 and $+\infty$ are:

$$\begin{cases} \lim_{G_* \rightarrow 0} H_1(G_*) = 2(a - b - d - \lambda), \\ \lim_{G_* \rightarrow +\infty} H_1(G_*) = -\infty. \end{cases} \quad (40)$$

Denote by H_2 the derivative of H_1 . We have $H_2(G_*) = 6c - \lambda(\alpha^3 G_*^2 + 6\alpha^2 G_* + 6\alpha)e^{\alpha G_*}$ and

$$\begin{cases} \lim_{G_* \rightarrow 0} H_2(G_*) = 6(c - \lambda\alpha), \\ \lim_{G_* \rightarrow +\infty} H_2(G_*) = -\infty. \end{cases} \quad (41)$$

We have $H_2'(G_*) = -\lambda(\alpha^4 G_*^2 + 8\alpha^3 G_* + 12\alpha)e^{\alpha G_*} < 0$. It implies that H_2 decreases.

(I) If $c - \lambda\alpha < 0$, then $H_2 < 0$. It means that H_1 decreases.

- 1) If $a - b - d - \lambda < 0$, then $H_1 < 0$. It implies that H' decreases. Using (39) and the intermediate value theorem, there exists a unique $G_{*1} \in]0, +\infty[$ such that $H'(G_{*1}) = 0$.
 - a) If $H(G_{*1}) < 0$, then there is no plausible savanna equilibrium.
 - b) If $H(G_{*1}) > 0$ and $a > b$, then there exists a unique savanna equilibrium $\mathbf{E}_* = (G_*, T_*)$ such that $G_* \in]G_{*1}, G^*[$.
 - c) If $H(G_{*1}) > 0$ and $a < b$, then there are two savanna equilibria: $\mathbf{E}_*^1 = (G_*^1, T_*^1)$ and $\mathbf{E}_*^2 = (G_*^2, T_*^2)$ such that $G_*^1 \in]0, G_{*1}[$ and $G_*^2 \in]G_{*1}, G^*[$.
- 2) If $a - b - d - \lambda > 0$, then using (40) and the intermediate value theorem, there exists a unique $G_{*2} \in]0, +\infty[$ such that $H_1(G_{*2}) = 0$. From (39) we have $H'(G_{*2}) > 0$. Then using (39) and the intermediate value theorem, there exists a unique $G_{*3} \in]G_{*2}, +\infty[$ such that $H'(G_{*3}) = 0$. Similarly as in 1) we have 0, 1, or 2 savanna equilibria.
 - a) If $H(G_{*3}) < 0$, then there is no plausible savanna equilibrium.
 - b) If $H(G_{*3}) > 0$ and $a > b$, then there exists a unique savanna equilibrium $\mathbf{E}_{**} = (G_{**}, T_{**})$ such that $G_{**} \in]G_{*3}, G^*[$.
 - c) If $H(G_{*3}) > 0$ and $a < b$, then there are two savanna equilibria: $\mathbf{E}_{**}^1 = (G_{**}^1, T_{**}^1)$ and $\mathbf{E}_{**}^2 = (G_{**}^2, T_{**}^2)$ such that $G_{**}^1 \in]0, G_{*3}[$ and $G_{**}^2 \in]G_{*3}, G^*[$.

(II) If $c - \lambda\alpha > 0$, then using (41) and the intermediate value theorem, there exists a unique $\bar{G}_{*1} \in]0, +\infty[$ such that $H_2(\bar{G}_{*1}) = 0$.

- 1) If $H_1(\bar{G}_{*1}) < 0$, then $H_1(G_*) < 0$. It implies that H' decreases. Using (39) and the intermediate value theorem, there exists a unique $\bar{G}_{*2} \in]0, +\infty[$ such that $H'(\bar{G}_{*2}) = 0$.
 - a) If $H(\bar{G}_{*2}) < 0$, then there is no plausible savanna equilibrium.
 - b) If $H(\bar{G}_{*2}) > 0$ and $a > b$, then there exists a unique savanna equilibrium $\bar{\mathbf{E}}_* = (\bar{G}_*, \bar{T}_*)$ such that $\bar{G}_* \in]\bar{G}_{*2}, G^*[$.
 - c) If $H(\bar{G}_{*2}) > 0$ and $a < b$, then there are two savanna equilibria: $\bar{\mathbf{E}}_*^1 = (\bar{G}_*^1, \bar{T}_*^1)$ and $\bar{\mathbf{E}}_*^2 = (\bar{G}_*^2, \bar{T}_*^2)$ such that $\bar{G}_*^1 \in]0, \bar{G}_{*2}[$ and $\bar{G}_*^2 \in]\bar{G}_{*2}, G^*[$.
- 2) If $H_1(\bar{G}_{*1}) > 0$ and $a - b - d - \lambda > 0$, then using (40) and the intermediate value theorem, there is $\bar{G}_{*3} \in]\bar{G}_{*2}, +\infty[$ such that $H_1(\bar{G}_{*3}) = 0$. Using (39) there exists $\bar{G}_{*4} \in]\bar{G}_{*3}, +\infty[$ such that $H'(\bar{G}_{*4}) = 0$.
 - a) If $H(\bar{G}_{*4}) < 0$, then there is no plausible savanna equilibrium.
 - b) If $H(\bar{G}_{*4}) > 0$ and $a > b$, then there exists a unique savanna equilibrium $\bar{\mathbf{E}}_{**} = (\bar{G}_{**}, \bar{T}_{**})$ such that $\bar{G}_{**} \in]\bar{G}_{*4}, G^*[$.

- c) If $H(\bar{G}_{*4}) > 0$ and $a < b$, then there are two savanna equilibria: $\bar{\mathbf{E}}_{**}^1 = (\bar{G}_{**}^1, \bar{T}_{**}^1)$ and $\bar{\mathbf{E}}_{**}^2 = (\bar{G}_{**}^2, \bar{T}_{**}^2)$ such that $\bar{G}_{**}^1 \in]0, \bar{G}_{*4}[$ and $\bar{G}_{**}^2 \in]\bar{G}_{*4}, G^*[$.
- 3) If $H_1(\bar{G}_{*1}) > 0$ and $a - b - d - \lambda < 0$, then using (40) and the intermediate value theorem there are $\bar{G}_{*5} \in]0, \bar{G}_{*1}[$ and $\bar{G}_{*6} \in]\bar{G}_{*1}, +\infty[$ such that $H_1(\bar{G}_{*5}) = 0 = H_1(\bar{G}_{*6})$.
- a) If $H'(\bar{G}_{*5}) > 0$ and $H'(\bar{G}_{*6}) > 0$, then using (39) and the intermediate value theorem there exists $\bar{G}_{*7} \in]\bar{G}_{*6}, +\infty[$ such that $H'(\bar{G}_{*7}) = 0$.
1. If $H(\bar{G}_{*7}) < 0$, then there is no plausible savanna equilibrium.
 2. If $H(\bar{G}_{*7}) > 0$ and $a > b$, then there exists a unique savanna equilibrium $\bar{\mathbf{E}}_{***} = (\bar{G}_{***}, \bar{T}_{***})$ such that $\bar{G}_{***} \in]\bar{G}_{*7}, G^*[$.
 3. If $H(\bar{G}_{*7}) > 0$ and $a < b$, then there are two savanna equilibria: $\bar{\mathbf{E}}_{***}^1 = (\bar{G}_{***}^1, \bar{T}_{***}^1)$ and $\bar{\mathbf{E}}_{***}^2 = (\bar{G}_{***}^2, \bar{T}_{***}^2)$ such that $\bar{G}_{***}^1 \in]0, \bar{G}_{*7}[$ and $\bar{G}_{***}^2 \in]\bar{G}_{*7}, G^*[$.
- b) If $H'(\bar{G}_{*5}) < 0$ and $H'(\bar{G}_{*6}) > 0$, then using (39) and the intermediate value theorem there are $\bar{G}_{*8} \in]0, \bar{G}_{*5}[$ and $\bar{G}_{*9} \in]\bar{G}_{*6}, +\infty[$ such that $H'(\bar{G}_{*8}) = 0 = H'(\bar{G}_{*9})$. Therefore, using (38) and the intermediate value theorem we have:
1. If $H(\bar{G}_{*8}) > 0$ and $a < b$, then there exist two savanna equilibria: $\bar{\mathbf{E}}_{****}^1 = (\bar{G}_{****}^1, \bar{T}_{****}^1)$ and $\bar{\mathbf{E}}_{****}^2 = (\bar{G}_{****}^2, \bar{T}_{****}^2)$ such that $\bar{G}_{****}^1 \in]0, \bar{G}_{*8}[$ and $\bar{G}_{****}^2 \in]\bar{G}_{*9}, G^*[$.
 2. If $(H(\bar{G}_{*8}) > 0$ and $a > b)$ or $(H(\bar{G}_{*8}) < 0, a < b, \text{ and } H(\bar{G}_{*9}) > 0)$, then there is a unique savanna equilibrium $\bar{\mathbf{E}}_{****} = (\bar{G}_{****}, \bar{T}_{****})$ such that $\bar{G}_{****} \in]\bar{G}_{*9}, G^*[$.
 3. If $H(\bar{G}_{*8}) < 0, a < b, \text{ and } H(\bar{G}_{*9}) < 0$, then there is no plausible savanna equilibrium.
 4. If $H(\bar{G}_{*8}) < 0, a > b, \text{ and } H(\bar{G}_{*9}) < 0$, then there is a unique savanna equilibrium $\bar{\mathbf{E}}_{*****} = (\bar{G}_{*****}, \bar{T}_{*****})$ such that $\bar{G}_{*****} \in]0, \bar{G}_{*8}[$.
 5. If $H(\bar{G}_{*8}) < 0, a > b, \text{ and } H(\bar{G}_{*9}) > 0$, there are three savanna equilibria: $\bar{\mathbf{E}}_{*****}^1 = (\bar{G}_{*****}^1, \bar{T}_{*****}^1)$, $\bar{\mathbf{E}}_{*****}^2 = (\bar{G}_{*****}^2, \bar{T}_{*****}^2)$, and $\bar{\mathbf{E}}_{*****}^3 = (\bar{G}_{*****}^3, \bar{T}_{*****}^3)$ such that $\bar{G}_{*****}^1 \in]0, \bar{G}_{*8}[$, $\bar{G}_{*****}^2 \in]\bar{G}_{*8}, \bar{G}_{*9}[$, and $\bar{G}_{*****}^3 \in]\bar{G}_{*9}, G^*[$.
- c) If $H'(\bar{G}_{*5}) < 0$ and $H'(\bar{G}_{*6}) < 0$, then using (39) and the intermediate value theorem there exists $\bar{G}_{*10} \in]0, \bar{G}_{*5}[$ such that $H'(\bar{G}_{*10}) = 0$. Using (38) and the intermediate value theorem we have:
1. If $H(\bar{G}_{*10}) < 0$, then there is no plausible savanna equilibrium.
 2. If $H(\bar{G}_{*10}) > 0$ and $a > b$, then there exists a unique savanna equilibrium $\bar{\mathbf{E}} = (\bar{G}, \bar{T})$ such that $\bar{G} \in]\bar{G}_{*10}, G^*[$.
 3. If $H(\bar{G}_{*10}) > 0$ and $a < b$, then there are two savanna equilibria: $\bar{\mathbf{E}}^1 = (\bar{G}^1, \bar{T}^1)$ and $\bar{\mathbf{E}}^2 = (\bar{G}^2, \bar{T}^2)$ such that $\bar{G}^1 \in]0, \bar{G}_{*10}[$ and $\bar{G}^2 \in]\bar{G}_{*10}, G^*[$.

Hence the theorem.

Appendix B: Proof of Theorem 3.3 (Stability of the savanna equilibrium)

From (??), the Jacobian matrix at the savanna equilibrium $\mathbf{E}_* = (G_*, T_*)$ is given by

$$J_* = J(G_*, T_*) = \begin{pmatrix} J_*^{11} & J_*^{12} \\ J_*^{21} & J_*^{22} \end{pmatrix},$$

where,

$$\begin{cases} J_*^{11} = g_G(\mathbf{W}) - (\delta_G + \lambda_f G f) - 2 \frac{g_G(\mathbf{W})}{K_G(\mathbf{W})} G_* - \eta_{TG} T_*, \\ J_*^{21} = -f \vartheta(T_*) \omega'(G_*) T_*, \\ J_*^{12} = -\eta_{TG} G_*, \\ J_*^{22} = g_T(\mathbf{W}) - \delta_T - 2 \frac{g_T(\mathbf{W})}{K_T(\mathbf{W})} T_* - f \omega(G_*) [\vartheta(T_*) + T_* \vartheta'(T_*)]. \end{cases} \quad (42)$$

The characteristic equation of J_* is

$$\mu^2 - \text{tr}(J_*)\mu + \det(J_*) = 0, \quad (43)$$

where, $\text{tr}(J_*) = J_*^{11} + J_*^{22}$ and $\det(J_*) = J_*^{11} J_*^{22} - J_*^{21} J_*^{12}$. It follows that all eigenvalues of characteristic equation have negative real part if and only if $\text{tr}(J_*) < 0$ and $\det(J_*) > 0$.

We have

$$\begin{aligned} \text{tr}(J_*) &= J_*^{11} + J_*^{22} \\ &= \frac{g_G(\mathbf{W})}{K_G(\mathbf{W})} (G^* - 2G_*) - \eta_{TG} T_* + \frac{g_T(\mathbf{W})}{K_T(\mathbf{W})} (T^* - 2T_*) - f \omega(G_*) [\vartheta(T_*) + T_* \vartheta'(T_*)] \\ &= \left\{ \frac{g_G(\mathbf{W})}{K_G(\mathbf{W})} G^* + \frac{g_T(\mathbf{W})}{K_T(\mathbf{W})} T^* - f \omega(G_*) \vartheta'(T_*) T_* \right\} \\ &\quad - \left\{ 2 \left(\frac{g_G(\mathbf{W})}{K_G(\mathbf{W})} G^* + \frac{g_T(\mathbf{W})}{K_T(\mathbf{W})} T^* \right) + \eta_{TG} T_* + f \omega(G_*) \vartheta(T_*) \right\} \\ &= \left\{ 2 \left(\frac{g_G(\mathbf{W})}{K_G(\mathbf{W})} G^* + \frac{g_T(\mathbf{W})}{K_T(\mathbf{W})} T^* \right) + \eta_{TG} T_* + f \omega(G_*) \vartheta(T_*) \right\} (\mathcal{R}_*^1 - 1), \end{aligned}$$

where,

$$\mathcal{R}_*^1 = \frac{\frac{g_G(\mathbf{W})}{K_G(\mathbf{W})} G^* + \frac{g_T(\mathbf{W})}{K_T(\mathbf{W})} T^* - f \omega(G_*) \vartheta'(T_*) T_*}{2 \left(\frac{g_G(\mathbf{W})}{K_G(\mathbf{W})} G^* + \frac{g_T(\mathbf{W})}{K_T(\mathbf{W})} T^* \right) + \eta_{TG} T_* + f \omega(G_*) \vartheta(T_*)}.$$

We have

$$\begin{aligned}
\det(J_*) &= J_*^{11} J_*^{22} - J_*^{21} J_*^{12} \\
&= \left[\frac{g_G(\mathbf{W})}{K_G(\mathbf{W})} (G^* - 2G_*) - \eta_{TG} T_* \right] \left[\frac{g_T(\mathbf{W})}{K_T(\mathbf{W})} (T^* - 2T_*) - f\omega(G_*) (\vartheta(T_*) + T_* \vartheta'(T_*)) \right] \\
&\quad - \eta_{TG} f\omega'(G_*) \vartheta(T_*) T_*^2 \\
&= \frac{g_G(\mathbf{W}) g_T(\mathbf{W})}{K_G(\mathbf{W}) K_T(\mathbf{W})} G^* T^* + \left(2 \frac{g_G(\mathbf{W})}{K_G(\mathbf{W})} G^* + \eta_{TG} T_* \right) \left(2 \frac{g_T(\mathbf{W})}{K_T(\mathbf{W})} T^* + f\omega(G_*) [\vartheta(T_*) + \vartheta'(T_*) T_*] \right) \\
&\quad - \frac{g_G(\mathbf{W})}{K_G(\mathbf{W})} G^* \left(2 \frac{g_T(\mathbf{W})}{K_T(\mathbf{W})} T^* + f\omega(G_*) [\vartheta(T_*) + \vartheta'(T_*) T_*] \right) - \frac{g_T(\mathbf{W})}{K_T(\mathbf{W})} T^* \left(2 \frac{g_G(\mathbf{W})}{K_G(\mathbf{W})} G^* + \eta_{TG} T_* \right) \\
&\quad - \eta_{TG} f\omega'(G_*) \vartheta(T_*) T_*^2 \\
&= \left(\frac{g_G(\mathbf{W})}{K_G(\mathbf{W})} G^* B_* + \frac{g_T(\mathbf{W})}{K_T(\mathbf{W})} T^* A_* + \eta_{TG} f\omega'(G_*) \vartheta(T_*) T_*^2 \right) (\mathcal{R}_*^2 - 1),
\end{aligned}$$

where,

$$A_* = 2 \frac{g_G(\mathbf{W})}{K_G(\mathbf{W})} G^* + \eta_{TG} T_*, \quad B_* = 2 \frac{g_T(\mathbf{W})}{K_T(\mathbf{W})} T^* + f\omega(G_*) [\vartheta(T_*) + \vartheta'(T_*) T_*], \text{ and}$$

$$\mathcal{R}_*^2 = \frac{\frac{g_G(\mathbf{W}) g_T(\mathbf{W})}{K_G(\mathbf{W}) K_T(\mathbf{W})} G^* T^* + A_* B_*}{\frac{g_G(\mathbf{W})}{K_G(\mathbf{W})} G^* B_* + \frac{g_T(\mathbf{W})}{K_T(\mathbf{W})} T^* A_* + \eta_{TG} f\omega'(G_*) \vartheta(T_*) T_*^2}.$$

Thus, the savanna equilibrium $\mathbf{E} = (G_*, T_*)$ is locally asymptotically stable if and only if $\mathcal{R}_*^1 < 1$ and $\mathcal{R}_*^2 > 1$. This ends the proof of theorem 3.3.

Appendix C: Brief overview of implementation of model (3) with MatCont

Upon the procedure of implementation of the bifurcation in Matcont (Dhooge et al., 2003; Dhooge et al., 2006), many steps are required. Below is the condensed overview of how one can use the software to implement the model.

- First, start to give numerical values to the parameters and the initial conditions in the Starter window of Matcont.
- The second step is to compute the orbits to explore the dynamics and find equilibria. Matcont window indicates an orbit point noted $P_O(1)$, meaning orbit number one which starts from the initial point. Choose the 2Dplot window in the Matcont window and put time on the abscissa and the variable T on the ordinate. In the Matcont window click on Forward to start the forward computation. One can explore the model, if necessary, by running orbits for different parameters and initial conditions.
- In step three, choose the Initial point item via Select in the Matcont window to see the initial points window. This lists the two orbits which have been run: $P_O(1)$ and $P_O(2)$. Then

select the last point of the last orbit that corresponds to the equilibrium of the current parameter settings. Now one can use the steady states found to draw the curve of the equilibrium as a function of one parameter.

- In step four, choose Equilibrium in the Initial point item of Select Type. Note that the Starter window changes and now contains the values of the last point of the orbit. One can now select the parameter over which to continue the equilibrium. Here, choose the fire frequency f .
- In step five, open a new 2Dplot window and draw the equilibrium curve over f . Compute both forward and backward to have the full equilibrium curve. Matcont indicates "LP (1)", "BP (1)" for forward and "LP (2)" and "BP (2)" for backward. Note that BP means "Branch point", which is the same thing as a transcritical bifurcation and LP means "Limit point", which refers to a saddle-node bifurcation.
- In step six, one can now continue the LP and BP bifurcations through the \mathbf{W} - f parameter space. That is draw the location of bifurcation as a function of two parameters. Then select for example the first LP point via Select and via Initial point. The new Starter window appears, in which one should keep parameters \mathbf{W} and f active. Computing both forward and backward, MatCont detects three cusp points "CP" labelled by the small empty circles in Fig. 3-(b). Each CP point means that there is an equilibrium point with a zero eigenvalue, which corresponds to the centre type point in the theory of bifurcations. Now select the first BP point. The forward computing draws the curve from the bottom CP point to the full square and the backward computing draws the curve from the same CP point to the empty square (see Fig. 3-(b)). Notice that the second BP point can not be continued since there is an equilibrium which has positive eigenvalues, which means that it can not converge.

References

- L. Abbadie, J. Gignoux, X. Roux, and M. Lepage. *Lamto: structure, functioning, and dynamics of a savanna ecosystem*, volume 179. Springer, 2006.
- F. Accatino and C. De Michele. Interpreting woody cover data in tropical and subtropical areas: Comparison between the equilibrium and the non-equilibrium assumption. *Eco. Comp.*, 25:60–67, 2016.
- F. Accatino, C. De Michele, R. Vezzoli, D. Donzelli, and R. J. Scholes. Tree–grass co-existence in savanna: interactions of rain and fire. *J. Theor. Biol.*, 267(2):235–242, 2010. doi: 10.1016/j.jtbi.2010.08.012.
- F. Accatino, K. Wiegand, D. Ward, and C. De Michele. Trees, grass, and fire in humid savannas-The importance of life history traits and spatial processes. *Ecol. Modell.*, 320:135–144, 2016.
- R. Anguelov, Y. Dumont, and J. M.-S. Lubuma. On nonstandard finite difference schemes in biosciences. *AIP Conf. Proc.*, 1487(1):212–223, 2012. doi: 10.1063/1.4758961. URL <http://scitation.aip.org/content/aip/proceeding/aipcp/10.1063/1.4758961>.
- S. Archibald, David P. Roy, W Brian, Van Wilgen, and R. J. Scholes. What limits fire? an examination of drivers of burnt area in southern africa. *Global Change Biol.*, 15(3):613–630, 2009.

- S. Archibald, R. J. Scholes, D. P. Roy, G. Roberts, and L. Boschetti. Southern african fire regimes as revealed by remote sensing. *Int. J. Wildland Fire*, 19(7):861–878, 2010.
- D. D. Bainov and P. S. Simeonov. *Impulsive differential equations: periodic solutions and applications*, volume 66. CRC Press, 1993.
- D. D. Bainov and P. S. Simeonov. *Impulsive differential equations: asymptotic properties of the solutions*, volume 28. World Scientific, 1995.
- N. Barbier, P. Couteron, R. Lefever, V. Deblauwe, and O. Lejeune. Spatial decoupling of facilitation and competition at the origin of gapped vegetation patterns. *Ecology*, 89(6):1521–1531, 2008.
- M. Baudena and M. Rietkerk. Complexity and coexistence in a simple spatial model for arid savanna ecosystems. *Theor. Ecol.*, 6(2):131–141, 2013.
- M. Baudena, F. D’Andrea, and A. Provenzale. An idealized model for tree-grass coexistence in savannas: the role of life stage structure and fire disturbances. *J. Ecol.*, 98:74–80, 2010.
- M. Baudena, S. C. Dekker, P. M. van Bodegom, B. Cuesta, S. I. Higgins, V. Lehsten, C. H. Reick, M. Rietkerk, S. Scheiter, Z. Yin, M. A. Zavala, and V. Brovkin. Forests, savannas and grasslands: bridging the knowledge gap between ecology and dynamic global vegetation models. *Biogeosci. Discuss.*, 11(6):9471–9510, 2014. doi: 10.5194/bgd-11-9471-2014.
- B. Beckage, W. Platt, and L. Gross. Vegetation, fire and feedbacks: a disturbance-mediated model of savannas. *Am. Nat.*, 174(6):805–818, 2009.
- B. Beckage, L.J. Gross, and W. J. Platt. Grass feedbacks on fire stabilize savannas. *Ecol. Modell.*, 222(14):2227–2233, 2011. doi: 10.1016/j.ecolmodel.2011.01.015.
- W. J. Bond. What limits trees in c4 grasslands and savannas? *Annu. Rev. Ecol. Evol. Syst.*, 39: 641–659, 2008.
- W. J. Bond and C. L. Parr. Beyond the forest edge: ecology, diversity and conservation of the grassy biomes. *Biol. Conserv.*, 143(10):2395–2404, 2010.
- W. J. Bond, F. I. Woodward, and G. F. Midgley. The global distribution of ecosystems in a world without fire. *New Phytol.*, 165(2):525–538, 2005.
- H. M. H Braun. Primary production in the serengeti: purpose, methods and some results of research. In *IBP regional meeting on Grasslands Research Projects (Lamto, Ivory Coast, 30.12.1971–3.1.1972)*, 1972a.
- H. M. H Braun. *Botanische samenstelling van de vegetaties in de Serengeti Plains. Typescript report to Wageningen University and the Serengeti Research Institute (in Dutch)*. 1972b.
- G. Bucini and N. P. Hanan. A continental-scale analysis of tree cover in african savannas. *Global Ecol. Biogeogr.*, 16:593–605, 2007.
- E. N Chidumayo. Above-ground woody biomass structure and productivity in a zambesian woodland. *For. Ecol. Manage.*, 36(1):33–46, 1990.

- A. Cuni-Sanchez, Lee J. T. White, Kim Calders, K. J. Jeffery, K. Abernethy, Andrew Burt, Mathias Disney, Martin Gilpin, Jose L Gomez-Dans, and Simon L Lewis. African savanna-forest boundary dynamics: A 20-year study. *PLoS One*, 11(6):e0156934, 2016.
- C. De Michele, R. Vezzoli, H. Pavlopoulos, and R. J. Scholes. A minimal model of soil water-vegetation interactions forced by stochastic rainfall in water-limited ecosystems. *Ecol. Modell.*, 212(3):397-407, 2008.
- C. De Michele, F. Accatino, R. Vezzoli, and R.J. Scholes. Savanna domain in the herbivores-fire parameter space exploiting a tree-grass-soil water dynamic model. *J. Theor. Biol.*, 289:74-82, 2011. doi: 10.1016/j.jtbi.2011.08.014.
- A. Dhooge, W. Govaerts, and Y. A. Kuznetsov. MATCONT: A MATLAB package for numerical bifurcation analysis of ODEs. *ACM TOMS*, 29(2):141-164, 2003.
- A. Dhooge, W. Govaerts, Y. A. Kuznetsov, W. Mestrom, A. M. Riet, and B. Sautois. *MATCONT and CL MATCONT: Continuation toolboxes in matlab*. Universiteit Gent, Belgium and Utrecht University, The Netherlands, 2006.
- A. Diouf, N. Barbier, A.M. Lykke, P. Couteron, V. Deblauwe, A. Mahamane, M. Saadou, and J. Bogaert. Relationships between fire history, edaphic factor and woody vegetation structure and composition in a semi-arid savanna landscape (niger, west africa). *Appl. Veg. Sci.*, 15:488-500, 2012.
- P. D’Odorico, F. Laio, and L. Ridolfi. A probabilistic analysis of fire-induced tree-grass coexistence in savannas. *Am. Nat.*, 167(3):E79-E87, 2006. doi: 10.1086/500617.
- C. Favier, J. Chave, A. Fabing, D. Schwartz, and M.A. Dubois. Modelling forest-savanna mosaic dynamics in man-influenced environments: effects of fire, climate and soil heterogeneity. *Ecol. Modell.*, 171(1):85-102, 2004. doi: 10.1016/j.ecolmodel.2003.07.003.
- C. Favier, J. Aleman, L. Bremond, M.A. Dubois, V. Freycon, and J.-M. Yangakola. Abrupt shifts in african savanna tree cover along a climatic gradient. *Global Ecol. Biogeogr.*, 21(8):787-797, 2012. doi: 10.1111/j.1466-8238.2011.00725.x.
- P. Frost, E. Medina, J. C. Menaut, O. Solbrig, M Swift, and B Walker. *Responses of savannas to stress and disturbance*. Biology International, 1986.
- R.E. Gaines and J.L. Mawhin. *Coincidence degree, and nonlinear differential equations*. Springer, 1977.
- W. Govaerts, R. K. Ghaziani, Yu. A. Kuznetsov, and H. G. E. Meijer. Numerical methods for two-parameter local bifurcation analysis of maps. *SIAM J. Sci. Comput.*, 29(6):2644-2667, 2007.
- N. Govender, W. S. W. Trollope, and B. W. Van Wilgen. The effect of fire season, fire frequency, rainfall and management on fire intensity in savanna vegetation in south africa. *J. Appl. Ecol.*, 43(4):748-758, 2006.

- S. I. Higgins, W. J. Bond, E. C. February, A. Bronn, D. I. W. Euston-Brown, B. Enslin, N. Govender, L. Rademan, S. O'Regan, A. L. F. Potgieter, S. Scheiter, R. Sowry, L. Trollope, and W. S. W. Trollope. Effects of four decades of fire manipulation on woody vegetation structure in savanna. *Ecology*, 88(5):1119–1125, 2007.
- S. I. Higgins, S. Scheiter, and M. Sankaran. The stability of african savannas: insights from the indirect estimation of the parameters of a dynamic model. *Ecology*, 91(6):1682–1692, 2010.
- S.I. Higgins, W.J. Bond, and W.S.W. Trollope. Fire, resprouting and variability: a recipe for grass–tree coexistence in savanna. *J. Ecol.*, 88(2):213–229, 2000. doi: 10.1046/j.1365-2745.2000.00435.x.
- R. J. Hijmans, S. E. Cameron, J. L. Parra, P. G. Jones, and A. Jarvis. Very high resolution interpolated climate surfaces for global land areas. *Int. J. Climatol.*, 25(15):1965–1978, 2005.
- M. Hirota, M. Holmgren, E. H. Van Nes, and M. Scheffer. Global resilience of tropical forest and savanna to critical transitions. *Science*, 334(6053):232–235, 2011.
- W. A. Hoffmann and O. T. Solbrig. The role of topkill in the differential response of savanna woody species to fire. *For. Ecol. Manage.*, 180(1):273–286, 2003.
- J. I. House, S. Archer, D. D. Breshears, and R. J. Scholes. Conundrums in mixed woody–herbaceous plant systems. *J. Biogeogr.*, 30(11):1763–1777, 2003.
- K. J. Jeffery, L. Korte, F. Palla, G. M. Walters, L. White, and K. Abernethy. *Fire management in a changing landscape: a case study from Lopé National Park, Gabon*, volume 20.1. International Union for Conservation of Nature and Natural Resources, 2014.
- R. Koenker and B. J. Park. An interior point algorithm for nonlinear quantile regression. *Journal of Econometrics*, 71(1):265–283, 1996.
- V. Lakshmikantham, D. Bainov, and P.S. Simeonov. *Theory of impulsive differential equations*, volume 6. World Scientific, 1989.
- X. Le Roux and T. Bariac. Seasonal variations in soil, grass and shrub water status in a west african humid savanna. *Oecologia*, 113(4):456–466, 1998.
- C. E. R. Lehmann, S. A. Archibald, W. A. Hoffmann, and W. J. Bond. Deciphering the distribution of the savanna biome. *New Phytol.*, 191(1):197–209, 2011.
- V. Lehsten, A. Arneth, A. Spessa, K. Thonicke, and A. Moustakas. The effect of fire on tree–grass coexistence in savannas: a simulation study. *Int. J. wildland fire*, 25(2):137–146, 2016.
- S. L. Lewis, B. Sonké, T. Sunderland, S. K. Begne, G. Lopez-Gonzalez, G. M. F. van der Heijden, O. L. Phillips, K. Affum-Baffoe, T. R. Baker, L. Banin, J. F. Bastin, H. Beeckman, P. Boeckx, J. Bogaert, C. De Cannière, E. Chezeaux, C. J. Clark, M. Collins, G. Djangbletey, M. N. K. Djuikouo, V. Droissart, J. L. Doucet, C. E. N. Ewango, S. Fauset, T. R. Feldpausch, E. G. Foli, J. F. Gillet, A. C. Hamilton, D. J. Harris, T. B. Hart, T. de Haulleville, A. Hladik, K. Hufkens, D. Huygens, P. Jeanmart, K. J. Jeffery, E. Kearsley, M. E. Leal, J. Lloyd, J. C. Lovett, J. R. Makana, Y. Malhi, A. R. Marshall, L. Ojo, K. S.-H. Peh, G. Pickavance, J. R. Poulsen, J. M. Reitsma, D. Sheil, M. Simo, H. E. Taedoung, J. Talbot, J. R. D. Taplin, D. Taylor, S. C. Thomas,

- B. Toirambe, H. Verbeeck, J. Vleminckx, L. J. T. White, S. Willcock, H. Woell, and L. Zomagho. Aboveground biomass and structure of 260 african tropical forests. *Phil. Trans. R. Soc. B.*, 368:20120295, 2013.
- R. Martínez-García, J. M. Calabrese, and C. López. Spatial patterns in mesic savannas: the local facilitation limit and the role of demographic stochasticity. *J. Theor. Biol.*, 333:156–165, 2013.
- MATLAB. *The Mathworks Inc.* <http://www.mathworks.com>.
- S. J. McNaughton. The propagation of disturbance in savannas through food webs. *J. Veg. Sci.*, 3(3):301–314, 1992.
- J. C. Menaut and J. Cesar. Structure and primary productivity of Lamto savannas, Ivory Coast. *Ecology*, pages 1197–1210, 1979.
- S. Mermoz, M. Réjou-Méchain, L. Villard, T. Le Toan, V. Rossi, and S. Gourlet-Fleury. Decrease of l-band sar backscatter with biomass of dense forests. *Remote Sens. Environ.*, 159:307–317, 2015.
- E. T. A. Mitchard and C. M. Flintrop. Woody encroachment and forest degradation in sub-saharan africa’s woodlands and savannas 1982–2006. *Phil. Trans. R. Soc. B*, 368(1625):20120406, 2013.
- E. T. A. Mitchard, S. S. Saatchi, F. F. Gerard, S. L. Lewis, and P. Meir. Measuring woody encroachment along a forest–savanna boundary in central africa. *Earth Interact.*, 13(8):1–29, 2009.
- P. Mordelet. *Influence des arbres sur la strate herbacée d’une savane humide(Lamto, Côte d’Ivoire)*. PhD thesis, 1993.
- A. Moustakas, William. E. Kunin, Tom. C. Cameron, and Mahesh Sankaran. Facilitation or competition? tree effects on grass biomass across a precipitation gradient. *PLoS One*, 8(2):e57025, 2013.
- F. W. T. Penning de Vries and M. A. Djitéye. *La productivité des pâturages sahéliens: une étude des sols, des végétations et de l’exploitation de cette ressource naturelle. (The productivity of Sahelian rangelands, a study of soils, vegetations, and exploitation of this natural resource.)*, volume 918. Agric. Res. Rep. (Versl. Landbouwk. Onderz.), 1982.
- M. Rietkerk, F. van den Bosch, and J. van de Koppel. Site-specific properties and irreversible vegetation changes in semi-arid grazing systems. *Oikos*, pages 241–252, 1997.
- M. Rietkerk, M. C. Boerlijst, F. van Langevelde, R. HilleRisLambers, J. van de Koppel, L. Kumar, H. H. T. Prins, and A. M. de Roos. Self-organization of vegetation in arid ecosystems. *Am. Nat.*, 160(4):524–530, 2002.
- M. Sankaran, N. P. Hanan, R. J. Scholes, J. Ratnam, D. J. Augustine, B. S. Cade, J. Gignoux, S. I. Higgins, X. Le Roux, F. Ludwig, J. Ardo, F. Banyikwa, A. Bronn, G. Bucini, K. K. Caylor, M. B. Coughenour, A. Diouf, W. Ekaya, C. J. Feral, E. C. February, P. G. H. Frost, P. Hiernaux, H. Hrabar, K. L. Metzger, H. H. T. Prins, S. Ringrose, W. Sea, J. Tews, Worden. J, and N. Zambatis. Determinants of woody cover in african savannas. *Nature*, 438(7069):846–849, 2005. doi:10.1038/nature04070.

- S. Scheiter. *Grass–tree interactions and the ecology of African savannas under current and future climates*. PhD thesis, 2009.
- S. Scheiter and S. I. Higgins. Partitioning of root and shoot competition and the stability of savannas. *Am. Nat.*, 179:587–601, 2007.
- R. J. Scholes. Convex relationships in ecosystems containing mixtures of trees and grass. *Environ. Resour. Econ.*, 26(4):559–574, 2003.
- R.J. Scholes and S. R. Archer. Tree-grass interactions in savannas. *Annu. Rev. Ecol. Evol. Syst.*, pages 517–544., 1997. doi: 10.1146/annurev.ecolsys.28.1.517.
- R.J. Scholes and B.H. Walker. *An African savanna: Synthesis of the Nylsvley study*. Cambridge University Press, 1993.
- G. Simioni, J. Gignoux, and X. Le Roux. Tree layer spatial structure can affect savanna production and water budget: results of a 3-d model. *Ecology*, 84(7):1879–1894, 2003.
- A. Carla. Staver, Sally. Archibald, and Simon. A. Levin. The global extent and determinants of savanna and forest as alternative biome states. *Science*, 334(6053):230–232, 2011a.
- A.C. Staver and S.A. Levin. Integrating theoretical climate and fire effects on savanna and forest systems. *Am. Nat.*, 180(2):211–224, 2012. doi: 10.1086/666648.
- A.C. Staver, S. Archibald, and S. Levin. Tree cover in sub-saharan africa: rainfall and fire constrain forest and savanna as alternative stable states. *Ecology*, 92(5):1063–1072, 2011b. doi: 10.2307/41151234.
- A. Tchuinté Tamen. *Study of a Generic Mathematical Model of Forest-Savanna Interactions: Case of Cameroon*. PhD thesis, University of Yaoundé I, 2017.
- A. Tchuinté Tamen, J. J. Tewa, P. Couteron, S. Bowong, and Y. Dumont. A generic modeling of fire impact in a tree-grass savanna model. *BIOMATH*, 3(2):1407191, 2014.
- A. Tchuinté Tamen, Y. Dumont, J. J. Tewa, S. Bowong, and P. Couteron. Tree–grass interaction dynamics and pulsed fires: Mathematical and numerical studies. *Appl. Math. Model.*, 40:6165–6197, 2016. doi: <http://dx.doi.org/10.1016/j.apm.2016.01.019>.
- A. Tchuinté Tamen, Y. Dumont, J. J. Tewa, S. Bowong, and P. Couteron. A minimalistic model of tree–grass interactions using impulsive differential equations and non-linear feedback functions of grass biomass onto fire-induced tree mortality. *Math. Comput. Simulation*, 133:265–297, 2017. doi: <http://dx.doi.org/10.1016/j.matcom.2016.03.008>.
- W. S. W Trollope, L. A. Trollope, and D. C. Hartnett. Fire behaviour a key factor in the fire ecology of african grasslands and savannas. *Forest Fire Research and Wildland Fire Safety, Viegas (ed.)*, Millpress, Rotterdam, 2002.
- UNESCO. Ecosystèmes pâturés tropicaux. Un rapport sur l’état des connaissances préparé par l’UNESCO, le PNUE et la FAO. In *Recherches sur les Ressources Naturelles, XVI*. Presses Univ. de France, Vendôme 675 p, 144 fig., 169 tabl., 1981.

- J. Van De Koppel and M. Rietkerk. Herbivore regulation and irreversible vegetation change in semi-arid grazing systems. *Oikos*, 90(2):253–260, 2000.
- J. van de Koppel, M. Rietkerk, and F. J. Weissing. Catastrophic vegetation shifts and soil degradation in terrestrial grazing systems. *Trends Ecol. Evol.*, 12(9):352–356, 1997.
- F. Van Langevelde, C.A.D.M. Van De Vijver, L. Kumar, J. Van De Koppel, N. De Ridder, J. Van Andel, A.K. Skidmore, J.W. Hearne, L. Stroosnijder, W.J. Bond, et al. Effects of fire and herbivory on the stability of savanna ecosystems. *Ecology*, 84(2):337–350, 2003.
- T. T. van Leeuwen, G. R. Van der Werf, A. A. Hoffmann, R. G. Detmers, G. Rücker, N. H. F. French, S. Archibald, J. A. Carvalho Jr, G. D. Cook, W. J. De Groot, C. Hély, E. C. Kasischke, S. Kloster, L. J. McCarty, M. L. Pettinari, P. Savadogo, E. C. Alvarado, L. Boschetti, S. Manuri, C. P. Meyer, F. Siegert, L. A. Trollope, and W. S. W. Trollope. Biomass burning fuel consumption rates: a field measurement database. *Biogeosciences*, 11:7305–7329, 2014.
- E. H. Van Nes, Marina Hirota, Milena Holmgren, and Marten Scheffer. Tipping points in tropical tree cover: linking theory to data. *Global Change Biol.*, 20(3):1016–1021, 2014.
- B.W. Van Wilgen, N. Govender, H.C. Biggs, D. Ntsala, and X.N. Funda. Response of savanna fire regimes to changing fire-management policies in a large african national park. *Conserv. Biol.*, 18(6):1533–1540, 2004. doi: 10.1111/j.1523-1739.2004.00362.x.
- B.H. Walker and I. Noy-Meir. Aspects of the stability and resilience of savanna ecosystems. In *Ecology of tropical savannas*, pages 556–590. Springer, 1982. doi: 10.1007/978-3-642-68786-0.
- B.H. Walker, D. Ludwig, C.S. Holling, and R.M. Peterman. Stability of semi-arid savanna grazing systems. *The Journal of Ecology*, pages 473–498, 1981.
- G. B. West, B. J. Enquist, and J. H. Brown. A general quantitative theory of forest structure and dynamics. *Proc. Natl. Acad. Sci.*, 106(17):7040–7045, 2009.
- R. H. Whittaker. *Communities and ecosystems*. . Second edition. Macmillan, New York, New York, USA, 1975.
- V. Yatat, Y. Dumont, J.J. Tewa, P. Couteron, and S. Bowong. Mathematical analysis of a size structured tree-grass competition model for savanna ecosystems. *BIOMATH*, 3(1):1404212, 2014.
- V. Yatat, P. Couteron, J. J. Tewa, S. Bowong, and Y. Dumont. An impulsive modelling framework of fire occurrence in a size-structured model of tree–grass interactions for savanna ecosystems. *J. Math. Biol.*, pages 1–58, 2016. doi: 10.1007/s00285-016-1060-y.
- K. Yu and P. D’Odorico. An ecohydrological framework for grass displacement by woody plants in savannas. *J. Geophys. Res. Biogeosci.*, 119(3):192–206, 2014.